DR IVY A. ROSALES (Orcid ID : 0000-0003-0621-3202)

DR ROBERT B COLVIN (Orcid ID : 0000-0002-4493-4150)

Article type : Original Article

Novel intragraft regulatory lymphoid structures in kidney allograft tolerance

Ivy A. Rosales[1], Chao Yang[2], Evan A. Farkash[3], Tameem Ashry[2], Jifu Ge[2], Imad Aljabban[2], Archana Ayyar[2], Dorothy Ndishabandi[1,2], Rebecca White[1], Elena Gildner[1], Jingjing Gong[7], Yan Liang[7], Fadi G. Lakkis[4], Volker Nickeleit[5], Paul S. Russell[2], Joren C. Madsen[2,6], Alessandro Alessandrini[2], Robert B. Colvin[1]

[1]Immunopathology Research Laboratory, Department of Pathology, Massachusetts General Hospital, Boston, MA 02114, United States
[2]Center for Transplantation Sciences, Department of Surgery, Massachusetts General Hospital, Boston, MA 02114, United States
[3]Department of Pathology, University of Michigan, Ann Arbor, MI 48109, United States
[4]Thomas E. Starzl Transplantation Institute and Departments of Surgery and Immunology, University of Pittsburgh School of Medicine, Pittsburgh, PA 15261, United States

This is the author manuscript accepted for publication and has undergone full peer review but has not been through the copyediting, typesetting, pagination and proofreading process, which may lead to differences between this version and the Version of Record. Please cite this article as doi: 10.1111/AJT.16880

This article is protected by copyright. All rights reserved

[5]Division of Nephropathology, Department of Pathology and Laboratory Medicine, The University of North Carolina, Chapel Hill, NC 27599, United States
[6]Division of Cardiac Surgery, Department of Surgery, Massachusetts General Hospital, Boston, MA 02114, United States
[7]NanoString Technologies, Inc. Seattle, WA, 98109 United States

I.R. and C.Y. and are co-first authors; A.A. and R.B.C. are co-senior and co-corresponding authors.

Correspondence

Alessandro Alessandrini, Center for Transplantation Sciences, Department of Surgery, Massachusetts General Hospital, Boston, MA, United States
Email: ALESSAND@HELIX.MGH.HARVARD.EDU

Robert B. Colvin, Immunopathology Research Laboratory, Department of Pathology, Massachusetts General Hospital, Boston, MA, United States
Email: COLVIN@HELIX.MGH.HARVARD.EDU

Abbreviations:

HEV	high endothelial venules
PVN	polyoma virus nephropathy/nephritis
RIP-LTα	rat insulin promoter lymphotoxin α
TLOs	tertiary lymphoid organs
TOLS	Treg-rich organized lymphoid structures

This article is protected by copyright. All rights reserved

ABSTRACT

Intragraft events thought to be relevant to the development of tolerance are here subjected to a comprehensive mechanistic study during long term spontaneous tolerance that occurs in C57BL/6 mice that receive life sustaining DBA/2 kidneys. These allografts rapidly develop periarterial Treg-rich organized lymphoid structures (TOLS) that form in response to class II but not to class I MHC disparity and form independently of lymphotoxin α and lymphotoxin β receptor pathways. TOLS form *in situ* in the absence of lymph nodes, spleen, and thymus. Distinctive transcript patterns are maintained over time in TOLS including transcripts associated with Treg differentiation, T cell checkpoint signaling, and Th2 differentiation. Pathway transcripts related to inflammation are expressed in early stages of accepted grafts but diminish with time, while B cell transcripts increase. Intragraft transcript patterns at one week post-transplant distinguish those from kidneys destined to be rejected, i.e. C57BL/6 allografts into DBA/2 recipients, from those that will be accepted. In contrast to inflammatory tertiary lymphoid organs (iTLOs) that form in response to chronic viral infection and transgenic *Lta* expression, TOLS lack high endothelial venules and germinal centers. TOLS represent a novel, pathogenetically important type of TLO that are *in situ* markers of regulatory tolerance.

INTRODUCTION

Intragraft events have been postulated to be important for the development of tolerance. Seminal studies demonstrated tolerogenic cells in mouse skin grafts could transfer tolerance to naïve recipients [1]. Lymph nodes have long been regarded as the source of these tolerogenic cells, rather than the graft itself [2]. Recent pathological studies of kidney allografts in mice with long term spontaneous tolerance revealed $CD3^{+}Foxp3^{+}$ periarterial nodular aggregates in the renal cortex [3-5]. We have termed these aggregates Treg-rich organized lymphoid structures (TOLS), representing a novel member of the regulatory tertiary lymphoid organ (rTLOs) family. Depletion of Foxp3+ cells promoted dissolution of these lymphoid structures [5] and abolition of tolerance, indicating

This article is protected by copyright. All rights reserved

that the Foxp3+ cells are necessary for their integrity and that the tolerance is regulatory. Furthermore, Tregs isolated from spontaneously accepted kidney allografts can transfer tolerance of a skin graft to naïve recipients [6].

Here we describe the pathologic and molecular characteristics of TOLS and the mechanisms of their formation. TOLS differ in anatomy, cell type, and gene expression from inflammatory TLOs, which are ectopic collections of T and B cells arising in non-lymphoid tissue due to chronic inflammation or tissue injury from rejection, infection, neoplasia and autoimmunity [7-11].

Materials and Methods

Mice

The C57BL/6J (B6, $H2^b$), DBA/2J (DBA, $H2^d$), C3H/HeJ (C3H, $H2^k$), B6.Foxp3-GFP, and B6.C-$H2^{d/bByJ}$ strains were purchased from Jackson Laboratories (Bar Harbor, ME). All mice were maintained under pathogen-free conditions in filter-top cages throughout the experiments with an automatic water system and were cared for according to methods approved by the American Association for the Accreditation of Laboratory Animal Care. Formalin fixed paraffin embedded (FFPE) tissue blocks from kidneys of Black Swiss mice infected with murine polyomavirus and sacrificed 4-20 weeks after infection were obtained from Dr. Volker Nickeleit. FFPE tissue blocks from kidneys of rat insulin promoter-lymphotoxin α (RIP-LTα) mice (B6, Thy1.2, H-2b) [12] were obtained through Dr. Fadi Lakkis.

Kidney transplantation

Kidney transplantation was performed in the same way described in a previous report [5]. In brief, kidney allografts were prepared with the cuff of aorta and inferior vena cava. Anastomoses were performed in an end-to-side manner. The ureter was anastomosed to the urinary bladder. Bilateral nephrectomy was also simultaneously performed. Kidneys from DBA/2 donors were spontaneously

This article is protected by copyright. All rights reserved

accepted by C57BL/6 recipients as evidenced by normal BUN levels at 1-week post-transplant and up to 60 weeks post-transplant. C57BL/6 kidneys transplanted into DBA/2 recipients showed elevated BUN levels at 1-week post transplant and were typically rejected in 10-14 days. One week samples from allograft kidneys that were destined to be accepted (DBA/2 to C57BL/6) were compared to one week samples from those destined to be rejected (C57BL/6 to DBA/2).

Histological and Immunopathological Analysis

Sagittal sections of allografts were fixed in formalin and sections were stained for H and E and PAS. TOLS were defined as an aggregate of mononuclear cells around an artery or arteriole and which upon immunohistochemical studies showed abundant Foxp3+ cells admixed with T cells, B cells, macrophages and dendritic cells. TOLS do not have B and T cell compartmentalization and germinal centers. TOLS do not have high endothelial venules (Table 1).

Routine immunohistochemistry using enzyme-conjugated antibodies was performed on paraffin embedded tissue sections to identify the cellular phenotype of TOLS using Foxp3 (FJK-16s, Invitrogen – ThermoFisher Scientific, Carlsbad, CA), individually and as double stain with CD3 (Polyclonal DAKO Agilent, Santa Clara, CA). Other stains included CD4 (4SM95 Invitrogen-Thermo Scientific, Carlsbad, CA), CD8 (4SM15 Invitrogen-Thermo Scientific, Carlsbad, CA), F4/80 (CI:A3-1 Abcam, Cambridge MA), Lyve-1 (Polyclonal, R&D Systems, Minneapolis, MN), PNAd (MECA-79, BD Biosciences, CA), Ki-67 (16A8 Biolegend, San Diego, CA), Pax5 (Polyclonal Novus Biologicals, Centennial, CO), PDCA-1 (BST2 120G8.04, Novus Biologicals, Centennial, CO), Siglec-H (23M15C8, Novus Biologicals, Centennial, CO), B220 (RA3-652 BD Biosciences, CA), CD138 (281-2 BD Biosciences, CA), Prox1 (EPR 19273 Abcam, Cambridge, MA), podoplanin (RTD4E10 Abcam, Cambridge, MA), LAP (Polyclonal, R&D Systems, Minneapolis, MN), CD21 (EP3093 Abcam, Cambridge, MA). Pathologic evaluation was done using an Olympus BX53 microscope (Olympus, Center Valley, PA) equipped with a digital camera (DP76, Olympus, CA). Immunofluorescence microscopy was performed using an immunofluorescent microscope (Eclipse 50i; Nikon, Tokyo,

This article is protected by copyright. All rights reserved

Japan) equipped with a digital camera (Spot RT KE; Diagnostics Instruments, Sterling Heights, MI). Whole slide scans were performed at 20x magnification (Aperio CS; Aperio, Vista, CA) and morphometric analysis was performed using Aperio Digital Pathology software (Leica Biosystems, Buffalo Grove, IL) image analysis algorithms.

NanoString RNA Analysis. mRNA was extracted from formalin fixed paraffin embedded kidney tissue samples of normal and allograft kidneys as described [13,14]. Gene expression was assessed with a comprehensive Mouse Cancer Immunology probe set, which includes 770 genes related to the immune system and major cell pathways, plus housekeeping genes. mRNA numbers were detected using the nCounter Max platform (NanoString Technologies, Seattle, WA). Normalized counts were analyzed with the NanoString nSolver software (NanoString Technologies, Seattle, WA). Cell type and pathway analysis were performed using built-in and custom pathways in the Advanced Analysis module.

Digital Spatial Protein Profiling. 5-micron thick sections were cut from paraffin blocks of grafts from autopsy and were incubated with fluorescent-labeled antibodies to Foxp3, pan-cytokeratin, and alpha-smooth muscle actin at 4°C overnight. On the second day, the slides were scanned on a GeoMx™ Digital Spatial Profiler instrument and regions of interest (ROI) were selected. Due to the fact that the anti-Foxp3 antibody used as morphology marker competed with the clone in the DSP panel, a secondary antigen retrieval was done to remove the Foxp3 fluorescent staining. The slides were incubated with a pre-commercial Mouse Immuno-Oncology panel of protein antibodies which contained photocleavable indexing oligonucleotides and immunofluorescent markers pan-cytokeratin, and smooth muscle actin at 4°C overnight. Syto83 was added to stain the nucleus at room temperature for 5 minutes before loading to the GeoMx™ DSP instrument. The pre-selected ROIs were aligned and oligonucleotide tags from ROIs were collected and quantitated using the

This article is protected by copyright. All rights reserved

NanoString nCounter Max instrument. Normalized counts were analyzed using GraphPad Prism 9 (GraphPad Software Inc., CA).

Statistical analysis

Results are given as the mean ± 95% C.I. Variables among groups were compared using Student's t test, with $p < 0.05$ considered significant. These analyses were performed with Prism versions 5 and 7 (GraphPad Software Inc., CA).

RESULTS

Characteristics of TOLS in accepted kidney allografts [Fig. 1,2]

In the first week after transplantation, accepted DBA/2 to C57BL/6 kidney allografts show widespread cortical interstitial infiltrates of T cells (Figure 1A) with focal collections around interlobular and arcuate arteries. At 2-3 weeks post-transplant, accepted grafts show progressive formation of peri-arterial Treg-rich organized lymphoid structures (TOLS). These are well-defined at 6-8 weeks, with a mean area of 1.7 ± 0.3 mm^2 in cross section. TOLS are round to oval structures in cross section and form periarterial sheaths when viewed in longitudinal sections. The arteries and arterioles are normal, although mononuclear cells can sometimes be present underneath the endothelium and within the wall of interlobular arteries. Cells at the periphery of TOLS can be dispersed, occasionally invading tubules. The remainder of the kidney is generally unremarkable. TOLS persist in tolerant recipients up to 60 weeks post-transplant (Figure 1D).

TOLS have a predominant population of CD4+ cells with numerous Foxp3+ cells and a minor component of CD8+ cells (Supplemental Figure 1A-C). B cells (Pax5+, B220+) (Supplemental Figure 1D, 1E) are intermixed with T cells and do not show distinct compartmentalization. Follicular B cells (Pax5+, B220+, CD21+) are detected at 6-8 weeks, but follicles and defined germinal centers are not detectable. Plasmacytoid dendritic cells (PDCA1+, SiglecH+ pDCs) are

This article is protected by copyright. All rights reserved

found along the periphery of TOLS (Supplemental Figure 1F), as well as CD11b+ cells, F4/80+ macrophages and CD138+ plasma cells. Podoplanin (Supplemental Figure 1G, 2B) and Lyve-1 (Supplemental Figure 1H) positive lymphatic channels form within TOLS and contain a heterogenous population of cells including Tregs, T cells, B cells, and plasmacytoid dendritic cells (Supplemental Figure 2C-H).

At 6 weeks post-transplant, TOLS are significantly enriched in Foxp3+ cells (53.8 ± 6.5% of CD3+ cells) when compared to periarteriolar sheaths (PALS) of spleens from the same recipients (23.1 ± 10.9% of the CD3+ cells; $p<0.01$) (Figure 2A, 2B). The Foxp3+ cells in TOLS express TGFβ-related latency associated peptide (LAP), a marker of activated Foxp3+ cells [15]. LAP in TOLS is expressed at higher frequency than in recipient spleens ($p<0.0001$) (Figure 2C, 2D). Foxp3+ cells in TOLS also show marked proliferative activity (>50% Ki67+), similar to Foxp3+ cells in the spleen from the same recipients. TOLS do not have high endothelial venules (HEVs) as evidenced by morphology and lack of MECA79+ vessels (an antibody to peripheral node addressin/PNAd) [10,16].

Digital Spatial Protein Profiling [Fig. 3]

To complement immunohistochemical analysis, we performed multiplex spatial protein quantification using the NanoString GeoMx Digital Spatial Profiler, by comparing TOLS with non-TOLS cortex from the same kidney sections. TOLS-specific differential expression is revealed for T cell (CD3e, CD8a, CD4), Treg (GITR, Foxp3) and T cell checkpoint molecules (Lag3, PD-1, Vista) at 1 week and 6-8 weeks post-transplant. This characteristic feature within the periarterial structures suggest the roles of T cell checkpoint and regulation in tolerance. Increased B cell (CD19, CD27) and dendritic cell (CD11c) molecules are also present in TOLS at both timepoints.

Dynamic transcript changes in accepted grafts over time [Fig. 4]

To determine molecular pathways involved in graft acceptance, we assessed

This article is protected by copyright. All rights reserved

bulk mRNA transcripts by NanoString nCounter analysis of kidney grafts at selected time points after transplantation. Accepted grafts at 1 week compared to long term accepted grafts show an increase in cell specific transcripts such as T cell ($p<0.000005$), CD8 T cell ($p<0.0000001$), cytotoxic cell ($p<0.00001$) and NK cell ($p<0.0002$) scores which diminish over time. In contrast, Treg cell scores rise early and are sustained. B cell scores ($p<0.0003$) show progressive increase over 60 weeks post transplant. T follicular regulatory (Tfr) cell score (*Bcl6, Cxcr5, Cxcl13, Foxp3)* parallels the B cell data. Individual genes associated with inflammatory cytokines, chemokines, and cytotoxic CD8 T cells are differentially expressed, but show a significant reduction by 40 to 60 weeks (Supplemental Figure 3).

Pathway analysis shows varying degrees of reduction in mean scores of inflammatory pathways in accepted graft samples over time. Several pathways were prominent initially, but then markedly diminished, including cytokine signaling, innate and adaptive immune systems, Toll like receptor signaling and apoptosis pathways. Treg differentiation pathway scores are less reduced. MHC Class II antigen and B cell receptor signaling pathways are not reduced over time.

Transcriptional analysis of kidney allograft samples of early acceptance versus early rejection [Fig. 5,6]

Rejecting grafts are allograft kidneys of DBA/2 recipients from C57BL/6 mice. This strain combination shows elevated BUN at 1 week post-transplant. In contrast, grafts that are destined to be tolerant are allograft kidneys of C57BL/6 recipients from DBA/2 mice, a strain combination that shows spontaneous acceptance and normal BUN at 1 week and up to 60 weeks post-transplant. Accepted and rejecting grafts at 1 week have similar histology of diffuse infiltrating leukocytes. Rejecting grafts do not form TOLS. There are similar levels of infiltrating leukocytes, as judged by *Cd45* transcripts, as well as T-cell, B-cell, NK cell and dendritic cell function scores, complement pathway and

This article is protected by copyright. All rights reserved

chemokine pathway scores.

Differential expression of individual genes shows accepted grafts have elevated transcripts related to Treg cells (*Foxp3, Tcf7, Ikzf1, Ikzf2, Cxcr3*), NK cells (*Klrd1, Klrc2, Cd244, Slamf6, Slamf7*) and B cells (*Cxcl13*). In contrast, grafts with early rejection have increased transcripts related to macrophages (*F13a1, Msr1, Clec4n, S100a8, Cxcl14)*, myeloid cells (*Cd33, Trem2, Fpr2*), and matrix (*Fn1, Ppbp)* (Figure 5). Elevation of *Klrd1* is due to a mutation in DBA/2, not present in B6 [17].

Pathways that are elevated in early acceptance compared with early rejection include T cell checkpoint signaling (p=0.02), Th2 differentiation (p=0.03), and mTOR signaling (p=0.01) and IFNγ (p=0.01). Pathways lower in grafts that will be accepted include IFNγ (p=0.01), Th1 differentiation (p=0.04), and MHC class I antigen presentation (p=0.04) as well as cytotoxic T cell (p<0.02), neutrophil (p<0.002) and pDC (p<0.002). Treg subtypes, as defined transcriptionally by Miragaia and colleagues [18] were assessed using custom cell type panels in the NanoString nCounter software. Accepted grafts at 1 week show elevated pan-Treg (p<0.001), central Treg (cTreg, p<0.000015), effector Treg (eTreg, p<0.000002) and tumor infiltrating Treg (Treg-tumor, p<0.00037), T cell (p<0.003), B cell (p<0.03) transcript scores, when compared to rejecting grafts at 1 week post transplant (Figure 6).

TOLS are Distinguished from Inflammatory Tertiary Lymphoid Organs (iTLOs) in the Kidney [Fig. 7,8]

TLOs in RIP-LTα transgenic mouse. The RIP-LTα transgenic mouse expresses LTα in kidney tubular cells and characteristically develops TLOs in the cortex [10,19]. Native kidneys from RIP-LTα mice show cortical interstitial (Figure 7A) and subcapsular nodular aggregates of T and B cells, with distinct B cell follicles and germinal centers (Figure 7B) and MECA-79+ HEVs (Figure 7C). Periarterial sheaths are not formed.

This article is protected by copyright. All rights reserved

TLOs in Polyomavirus Nephropathy. Mice infected with murine polyomavirus develop interstitial nephritis over several weeks, and TLOs in the cortical parenchyma. The TLOs are randomly distributed in the cortex without specific localization, although some periarterial aggregates are present. The TLOs are associated with marked tubular injury and presence of epithelial nuclear viral inclusions. Numerous plasma cells in clusters are predominant, admixed with CD4+, CD8+ and B220+ cells. T cells and B cells are in distinct compartments and germinal centers are evident as well as HEV.

The level of *Cd45* transcripts is not significantly different in allograft kidneys with TOLS at 40-60 weeks compared to native kidneys with TLOs due to LTA Tg or PVN. However, transcripts related to Tregs, B cells, cytotoxic cells, macrophages and NK cells are increased in kidneys with TOLS.

Transcript analysis shows several differences between kidneys with TOLS and those with TLOs. TOLS show elevated pathways of Treg, T cell checkpoint signaling and Th2 differentiation, T and B cell receptor signaling, MHC Class I and II antigen presentation, and interferon signaling pathways compared with kidneys with TLOs due to either LTA Tg or PVN (Figure 8). Higher levels of pathway transcripts related to Th1 and Th17 cell function and TNF and NF-κB signaling characterize kidney with TLOs due to LTA Tg compared with PVN.

Accepted kidney allografts with TOLS also have increased transcripts that correlate with cTreg, eTreg and non-lymphoid tissue infiltrating Treg (NLT-Treg) compared with native kidneys with TLOs. Normal thymus and spleens have higher cTreg than accepted grafts with TOLS. Accepted grafts also have higher levels of eTreg and tissue infiltrating Treg, including those associated with tumors (Supplemental Figure 4).

Mechanisms of TOLS Formation [Fig. 9]

This article is protected by copyright. All rights reserved

Antigenic Stimulus. TOLS do not develop in syngeneic kidney grafts (B6 to B6), indicating allogeneic stimulation is necessary for their formation [5]. To test whether MHC Class I or Class II antigenic differences are sufficient to induce TOLS formation, B6.C-H-2^{bm1} (bm1) and B6.C-H-2^{bm12} (bm12) kidneys[20] were transplanted to wild type C57BL/6 recipients and analyzed 56 days post-transplant at a time when the serum creatinine was normal. Well-formed TOLS developed in bm12 kidney allografts, but not bm1 kidney allografts, which had minimal perivascular infiltrates along a few arcuate arteries and arterioles (Figure 9B).

Role of Lymphotoxin β *Signaling*. To test the dependence of TOLS on LTα or LTβ, we treated recipient animals with antagonistic LTβR-Ig for 28 days, using a dose schedule that is known to inhibit TLO induction [21,22]. This regimen did not inhibit TOLS formation in kidney allografts at 28 days. Bulk transcript pathway analysis showed no quantitative differences compared to wild type C57BL/6 recipients (data not shown). These data indicate that the LTβR signaling pathway, which is necessary for formation of TLOs[21,22], is dispensable in formation of TOLS (Figure 9C).

Role of Primary and Secondary Lymphoid Organs. The site of development of peripheral Foxp3+ T cells has long been considered to be secondary lymphoid organs [2,23]. To test whether lymph nodes are also necessary for development of TOLS, kidneys from DBA/2 were transplanted into C57BL/6 LTα KO mice, which fail to develop lymph nodes and cannot form TLOs[24]. Kidney allografts were spontaneously accepted. The histology showed well-formed TOLS at 56 days post-transplant in the absence of identifiable lymph nodes in the recipient. Bulk transcript pathway analysis showed no quantitative differences compared to wild type C57BL/6 recipients (data not shown). Similar results were observed in splenectomized C57BL/6 LTα KO mice recipients (Figure 9D). TOLS also form in DBA/2 kidneys in thymectomized C57BL/6 recipients which are accepted long-term (Figure 9E). These results indicate that spontaneous acceptance and

This article is protected by copyright. All rights reserved

formation of TOLS are independent of lymph node, spleen and thymic presence and function.

DISCUSSION

We have shown that the lymphoid infiltrates in accepted kidney allografts, which we refer to as TOLS, are novel members of regulatory tertiary lymphoid organs (rTLO) and are distinct from lymphoid infiltrates associated with chronic inflammation and rejection (iTLOs). There are similarities in the cellular makeup of TOLS and TLOs such as the presence of B and T cells, Tregs, conventional and plasmacytoid DCs, CD11b+ cells and plasma cells. However, among the differences seen in TOLS are lack of high endothelial venules and germinal centers and a well-defined anatomical distribution along small arteries. Joshi and colleagues have recently described TLOs that are associated with the tumor microenvironment of lung cancers in mice that, like TOLS, are regulatory in nature. But these structures differ from TOLS in that they exhibit CD31+PNAd+ HEV-like structures with distinct B and T cell zones [25]. Li and colleagues have described HEV+ bronchus-associated lymphoid tissue (BALT) that are regulatory in nature in mouse lung allografts, following the induction of tolerance by costimulatory blockade [26]. These have been termed BALT but a periarterial distribution has been illustrated, similar to TOLS.

The Foxp3+ cells in TOLS have a high proliferative rate and express LAP more abundantly than those in the spleen. Since Foxp3 cells are essential for the maintenance of TOLS and tolerance, as previously reported [5], and the *in vitro* induction of Foxp3 cells is dependent on class II and not class I MHC disparity [27], we hypothesized that class II MHC disparity would be the likely stimulus. Indeed, isolated class II mismatch (bm12 to B6) was sufficient to stimulate the formation of TOLS, which did not occur in class I mismatched allografts or isografts.

This article is protected by copyright. All rights reserved

While TOLS lack HEV, they develop prominent Lyve+Prox-1+Podoplanin+ lymphatic structures. Lymphatics are normally present in the kidney along the arterial tree and transport fluid and cells to regional lymph nodes. The expansion of lymphatic vessels within the TOLS may be important in the egress of lymphocytes and maintenance of tolerance. This fits with the recent study of Pedersen and colleagues who reported that the induction of lymphangiogenesis in kidney allografts in mice resulted in increased survival of the graft [28].

Several studies have implicated the lymphotoxin β receptor signaling pathway in the development of both lymph nodes and TLOs, as demonstrated by lack of lymph nodes and inducible TLOs in LTα KO, LTβ KO and LTβR KO mice[21,22,24] and absence of TLOs in chronically rejecting heart allografts[29]. Transplantation of DBA/2 kidneys into C57BL/6 LTα KO mice, with and without splenectomy, showed spontaneous acceptance of kidney grafts and TOLS formation. To further eliminate the possibility that donor kidneys are the source of lymphotoxin to activate LTβR signaling, recipient animals were treated with antagonistic LTβR-Ig for 28 days. There was spontaneous acceptance of kidney allografts and TOLS appeared normally.

The differences detected by transcripts between early rejection and early tolerance not only provides distinguishing characteristics but also reveals transcripts involved in early TOLS formation. The early presence of *Tcf7, Foxp3 Ikzf1* suggest early T cell differentiation into a regulatory phenotype. Bulk transcript analysis also suggests that increased T cell checkpoint signaling, Th2 differentiation and mTOR signaling pathways may be important in the genesis of tolerance. Transcripts associated with macrophages and myeloid cells indicate the role of innate immune cells in rejection or their downregulation during early acceptance. Our analysis using the GeoMx digital spatial profiler confirmed protein expression of Foxp3, GITR, and PD-1 in cells within TOLS as early as 1

This article is protected by copyright. All rights reserved

week, validating our findings from bulk transcript analysis, as well as T cell checkpoint and B cell protein markers.

One of the controversies in transplantation is the site where peripheral induction of Foxp3+ cells takes place, with considerable evidence that induction occurs in lymph nodes [23]. However, the lack of dependence on lymph nodes and spleen in the present model argues that the induction of Foxp3+ cells can occur in the allograft itself [30]. We show a high rate of proliferation of the Foxp3+ cells in TOLS, but we have no direct proof that Foxp3+ cells arise in the TOLS from non-Foxp3+ cells. We do show that this form of tolerance does not require the continued presence of the thymus for the generation of natural Tregs [31].

Tolerance is manifested in the graft by a progressive shift from cytotoxic/CD8 cells to Treg/CD4 cells and B cells. The time dependent induction of B cell-specific genes and protein markers in the accepted mouse kidney allografts are consistent with previous reports in human studies that renal transplant acceptance is associated with a B cell signature [32-34]. Many transcripts (n=130) in 1-week samples were significantly reduced at 40-60 weeks, including a variety of transcripts related to cytokines, chemokines, and cytotoxic CD8 T cells. Over time Foxp3 transcripts persist at high levels and MHC class II antigen presentation and B cell receptor signaling pathways were not reduced.

Transcripts characteristic of Treg subtypes, specifically cTreg, eTreg, and tumor infiltrating Tregs, show a sustained level of expression following kidney allograft transplantation. Interestingly, the Tfr signature mirrors that of B cells, showing an increased expression of transcripts specific for Tfr cells with time. What the relationship between Tfr and B cells is, especially in the context of the Tfh signature, which also parallels that of Tfr and B cells, is a focus of future studies. One possibility is that there is an interplay between these cells, mediating the function of B cells to a more regulatory phenotype and less so towards one that favors the development of anti-donor antibody producing plasma cells.

This article is protected by copyright. All rights reserved

This study has several limitations. Only 2 forms of TLOs were included and there is probably substantial heterogeneity of the phenotype. Nonetheless, consistent differences in TOLS were detected that probably apply to at least some TLOs. Furthermore, TOLS themselves may be heterogeneous. Foxp3+ rich aggregates in neoplasia have been reported to have HEV [25]. One report of TOLS in murine kidney grafts described HEV as judged by immunohistochemistry [35]. Similar results were observed by Tse and colleagues in a bm12 to B6 kidney transplant model using unilaterally nephrectomized recipients, where they observed HEV and chronic allograft damage[36]. In confirmation, we found that keeping a native kidney in B6 recipients of DBA/2 allografts led to histologic signs of rejection by 30 to 40 days post-transplant and development of HEV (unpublished data).

Our study did not establish the generality of TOLS in other conditions of tolerance. However, we have observed aggregates similar to murine TOLS in renal allografts in non-human primates with tolerance induced by mixed chimerism [37]. While Foxp3+ cells are critical for maintaining TOLS and preventing rejection[5], further studies will be needed to determine whether these intragraft structures *per se* mediate or predict outcomes and if the presence of HEV predicts susceptibility to future rejection episodes.

In conclusion, we have identified novel regulatory lymphoid organs, TOLS, in renal allografts in tolerant recipients that can be distinguished anatomically, phenotypically and genetically from other ectopic lymphoid structures that are inflammatory in nature, iTLOs. The formation of TOLS is dependent on class II MHC differences and does not require generation of Foxp3+ cells in lymph nodes, spleen or thymus. Foxp3+ cell proliferate in TOLS and we hypothesize that TOLS are the site of Foxp3+ induction, functionally different from iTLOs, and a marker of regulatory tolerance.

This article is protected by copyright. All rights reserved

Acknowledgments

This work was supported by US National Institutes of Health Grants P01-AI123086 (A.A., R.B.C., J.C.M.), T32-AI007529 (E.A.F.) and R01-AI081734 (R.B.C.). T.A. was supported by King Saud University College of Medicine, Department of Pathology, Riyadh, Saudi Arabia.

Disclosure

The authors of this manuscript have no conflicts of interest to disclose as described by the *American Journal of Transplantation.*

ORCID

Ivy A. Rosales	0000-0003-0621-3202
Chao Yang	0000-0002-0924-5915
Evan A. Farkash	0000-0002-5136-079X
Tameem Ashry	0000-0003-0616-7509
Jifu Ge	0000-0002-0989-4616
Imad Aljabban	0000-0003-1231-1159
Archana Ayyar	0000-0002-2779-5216
Dorothy Ndishabandi	0000-0003-2985-8783
Rebecca White	0000-0003-4935-0055
Elena Gildner	0000-0001-7003-6584
Jingjing Gong	0000-0002-5457-3686
Yan Liang	0000-0002-8536-5951
Fadi G. Lakkis	0000-0001-9937-2637
Volker Nickeleit	0000-0001-9997-286X
Paul S. Russell	0000-0002-1275-7348
Joren C. Madsen	0000-0003-2724-1333

This article is protected by copyright. All rights reserved

Alessandro Alessandrini 0000-0003-0347-1927
Robert B. Colvin 0000-0002-4493-4150

REFERENCES

1. Graca L, Cobbold SP, Waldmann H. Identification of regulatory T cells in tolerated allografts. *The Journal of experimental medicine.* Jun 17 2002;195(12):1641-1646.

2. Shevach EM. Foxp3(+) T Regulatory Cells: Still Many Unanswered Questions-A Perspective After 20 Years of Study. *Front Immunol.* 2018;9:1048.

3. Russell PS, Chase CM, Colvin RB, Plate JM. Induced immune destruction of long-surviving, H-2 incompatible kidney transplants in mice. *The Journal of experimental medicine.* May 1 1978;147(5):1469-1486.

4. Cook CH, Bickerstaff AA, Wang JJ, et al. Spontaneous renal allograft acceptance associated with "regulatory" dendritic cells and IDO. *J Immunol.* Mar 1 2008;180(5):3103-3112.

5. Miyajima M, Chase CM, Alessandrini A, et al. Early acceptance of renal allografts in mice is dependent on foxp3(+) cells. *The American journal of pathology.* Apr 2011;178(4):1635-1645.

6. Hu M, Wang C, Zhang GY, et al. Infiltrating Foxp3(+) regulatory T cells from spontaneously tolerant kidney allografts demonstrate donor-specific tolerance. *Am J Transplant.* Nov 2013;13(11):2819-2830.

7. Wang Z, Lyu Z, Pan L, Zeng G, Randhawa P. Defining housekeeping genes suitable for RNA-seq analysis of the human allograft kidney biopsy tissue. *BMC Med Genomics.* Jun 17 2019;12(1):86.

8. Hsiao HM, Li W, Gelman AE, Krupnick AS, Kreisel D. The Role of Lymphoid Neogenesis in Allografts. *Am J Transplant.* Apr 2016;16(4):1079-1085.

9. Drayton DL, Liao S, Mounzer RH, Ruddle NH. Lymphoid organ development: from ontogeny to neogenesis. *Nat Immunol.* Apr 2006;7(4):344-353.

10. Ruddle NH. High Endothelial Venules and Lymphatic Vessels in Tertiary Lymphoid Organs: Characteristics, Functions, and Regulation. *Front Immunol.* 2016;7:491.

11. Koenig A, Thaunat O. Lymphoid Neogenesis and Tertiary Lymphoid Organs in Transplanted Organs. *Front Immunol.* 2016;7:646.

This article is protected by copyright. All rights reserved

12. Picarella DE, Kratz A, Li CB, Ruddle NH, Flavell RA. Insulitis in transgenic mice expressing tumor necrosis factor beta (lymphotoxin) in the pancreas. *Proc Natl Acad Sci U S A.* Nov 1 1992;89(21):10036-10040.

13. Smith RN, Matsunami M, Adam BA, et al. RNA expression profiling of nonhuman primate renal allograft rejection identifies tolerance. *Am J Transplant.* Jun 2018;18(6):1328-1339.

14. Adam BA, Smith RN, Rosales IA, et al. Chronic Antibody-Mediated Rejection in Nonhuman Primate Renal Allografts: Validation of Human Histological and Molecular Phenotypes. *Am J Transplant.* Nov 2017;17(11):2841-2850.

15. Tran DQ, Andersson J, Hardwick D, Bebris L, Illei GG, Shevach EM. Selective expression of latency-associated peptide (LAP) and IL-1 receptor type I/II (CD121a/CD121b) on activated human FOXP3+ regulatory T cells allows for their purification from expansion cultures. *Blood.* May 21 2009;113(21):5125-5133.

16. Girard JP, Moussion C, Forster R. HEVs, lymphatics and homeostatic immune cell trafficking in lymph nodes. *Nat Rev Immunol.* Nov 2012;12(11):762-773.

17. Shin DL, Pandey AK, Ziebarth JD, et al. Segregation of a spontaneous Klrd1 (CD94) mutation in DBA/2 mouse substrains. *G3 (Bethesda).* Dec 17 2014;5(2):235-239.

18. Miragaia RJ, Gomes T, Chomka A, et al. Single-Cell Transcriptomics of Regulatory T Cells Reveals Trajectories of Tissue Adaptation. *Immunity.* Feb 19 2019;50(2):493-504 e497.

19. Kratz A, Campos-Neto A, Hanson MS, Ruddle NH. Chronic inflammation caused by lymphotoxin is lymphoid neogenesis. *J Exp Med.* Apr 1 1996;183(4):1461-1472.

20. Ishii D, Rosenblum JM, Nozaki T, et al. Novel CD8 T cell alloreactivities in CCR5-deficient recipients of class II MHC disparate kidney grafts. *J Immunol.* Oct 1 2014;193(7):3816-3824.

21. Browning JL, Allaire N, Ngam-Ek A, et al. Lymphotoxin-beta receptor signaling is required for the homeostatic control of HEV differentiation and function. *Immunity.* Nov 2005;23(5):539-550.

22. Tang H, Zhu M, Qiao J, Fu YX. Lymphotoxin signalling in tertiary lymphoid structures and immunotherapy. *Cell Mol Immunol.* Oct 2017;14(10):809-818.

This article is protected by copyright. All rights reserved

23. Ochando JC, Yopp AC, Yang Y, et al. Lymph node occupancy is required for the peripheral development of alloantigen-specific Foxp3+ regulatory T cells. *J Immunol.* Jun 1 2005;174(11):6993-7005.

24. Futterer A, Mink K, Luz A, Kosco-Vilbois MH, Pfeffer K. The lymphotoxin beta receptor controls organogenesis and affinity maturation in peripheral lymphoid tissues. *Immunity.* Jul 1998;9(1):59-70.

25. Joshi NS, Akama-Garren EH, Lu Y, et al. Regulatory T Cells in Tumor-Associated Tertiary Lymphoid Structures Suppress Anti-tumor T Cell Responses. *Immunity.* Sep 15 2015;43(3):579-590.

26. Li W, Gauthier JM, Higashikubo R, et al. Bronchus-associated lymphoid tissue-resident Foxp3+ T lymphocytes prevent antibody-mediated lung rejection. *J Clin Invest.* Feb 1 2019;129(2):556-568.

27. Oh NA, O'Shea T, Ndishabandi DK, et al. Plasmacytoid Dendritic Cell-driven Induction of Treg Is Strain Specific and Correlates With Spontaneous Acceptance of Kidney Allografts. *Transplantation.* Jan 2020;104(1):39-53.

28. Pedersen MS, Muller M, Rulicke T, et al. Lymphangiogenesis in a mouse model of renal transplant rejection extends life span of the recipients. *Kidney Int.* Jan 2020;97(1):89-94.

29. Motallebzadeh R, Rehakova S, Conlon TM, et al. Blocking lymphotoxin signaling abrogates the development of ectopic lymphoid tissue within cardiac allografts and inhibits effector antibody responses. *FASEB J.* Jan 2012;26(1):51-62.

30. Savage TM, Shonts BA, Obradovic A, et al. Early expansion of donor-specific Tregs in tolerant kidney transplant recipients. *JCI Insight.* Nov 15 2018;3(22).

31. Yang C, Ge J, Rosales I, et al. Kidney-induced systemic tolerance of heart allografts in mice. *JCI Insight.* Sep 17 2020;5(18).

32. Cherukuri A, Salama AD, Mehta R, et al. Transitional B cell cytokines predict renal allograft outcomes. *Sci Transl Med.* Feb 24 2021;13(582).

33. Newell KA, Adams AB, Turka LA. Biomarkers of operational tolerance following kidney transplantation - The immune tolerance network studies of spontaneously tolerant kidney transplant recipients. *Hum Immunol.* May 2018;79(5):380-387.

34. Newell KA, Asare A, Kirk AD, et al. Identification of a B cell signature associated with renal transplant tolerance in humans. *J Clin Invest.* Jun 2010;120(6):1836-1847.

This article is protected by copyright. All rights reserved

35. Brown K, Sacks SH, Wong W. Tertiary lymphoid organs in renal allografts can be associated with donor-specific tolerance rather than rejection. *European journal of immunology.* Jan 2011;41(1):89-96.

36. Tse GH, Johnston CJ, Kluth D, et al. Intrarenal B Cell Cytokines Promote Transplant Fibrosis and Tubular Atrophy. *Am J Transplant.* Dec 2015;15(12):3067-3080.

37. Matsunami M, Rosales IA, Adam BA, et al. Long-term Kinetics of Intragraft Gene Signatures in Renal Allograft Tolerance Induced by Transient Mixed Chimerism. *Transplantation.* Nov 2019;103(11):e334-e344.

Supporting Information

Additional supporting information may be found online in the Supporting Information section at the end of the manuscript.

This article is protected by copyright. All rights reserved

Figure 1

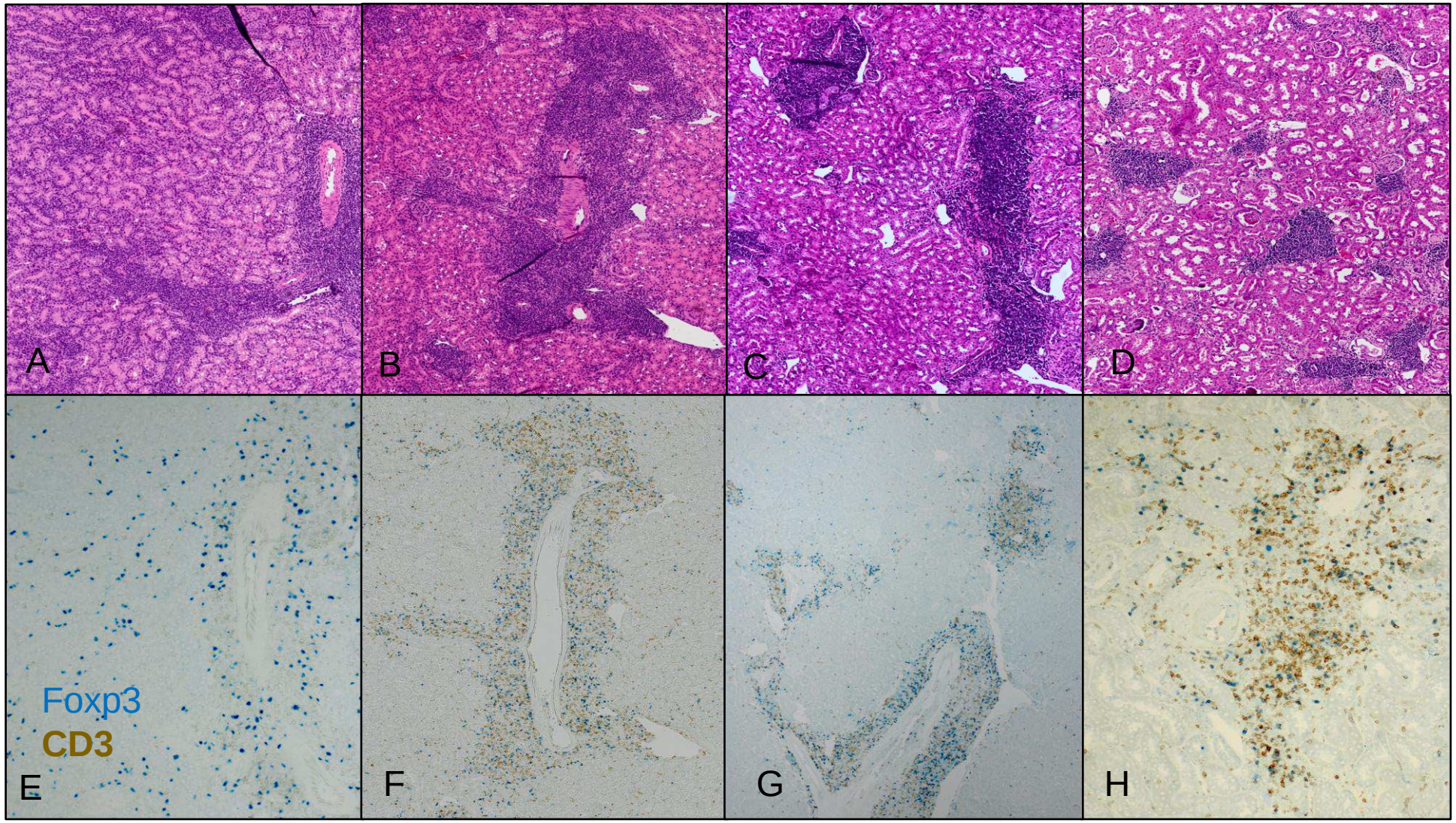

This article is protected by copyright. All rights reserved

Figure 2

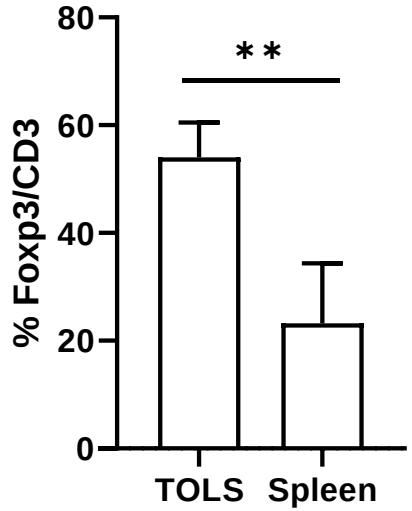

n = 8

A

%Foxp3+CD3+ cells in TOLS and spleens from same recipients

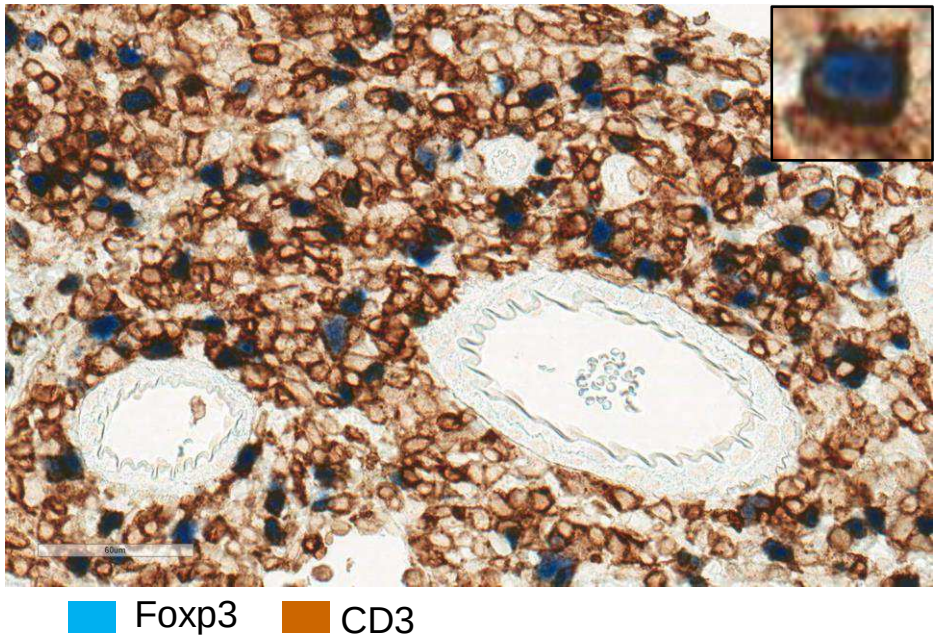

B

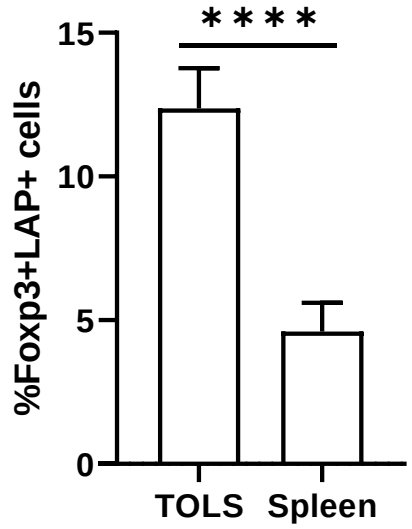

n = 7

C

%Foxp3+LAP+ cells in TOLS and spleens from same recipients

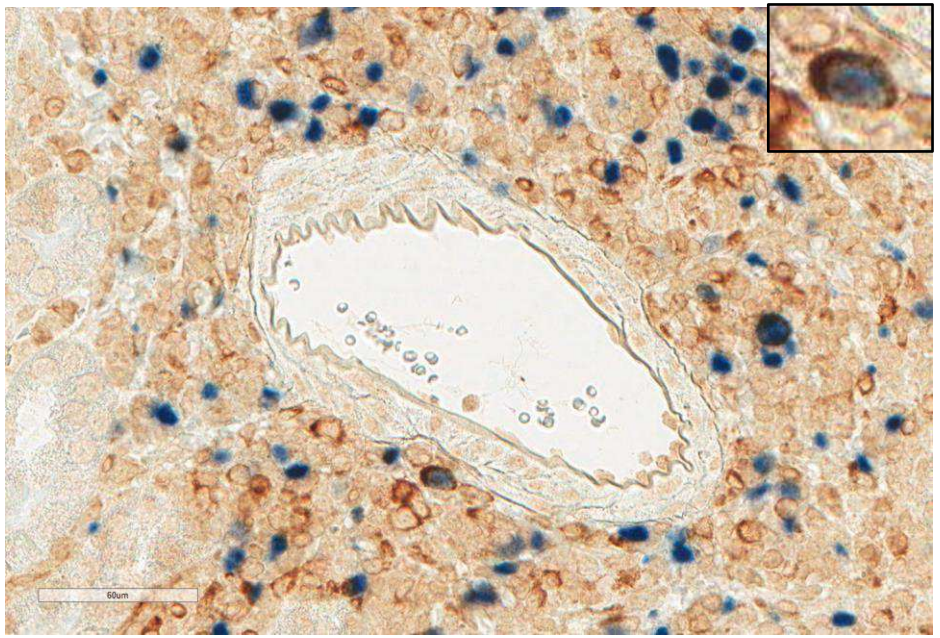

D

This article is protected by copyright. All rights reserved

Figure 3

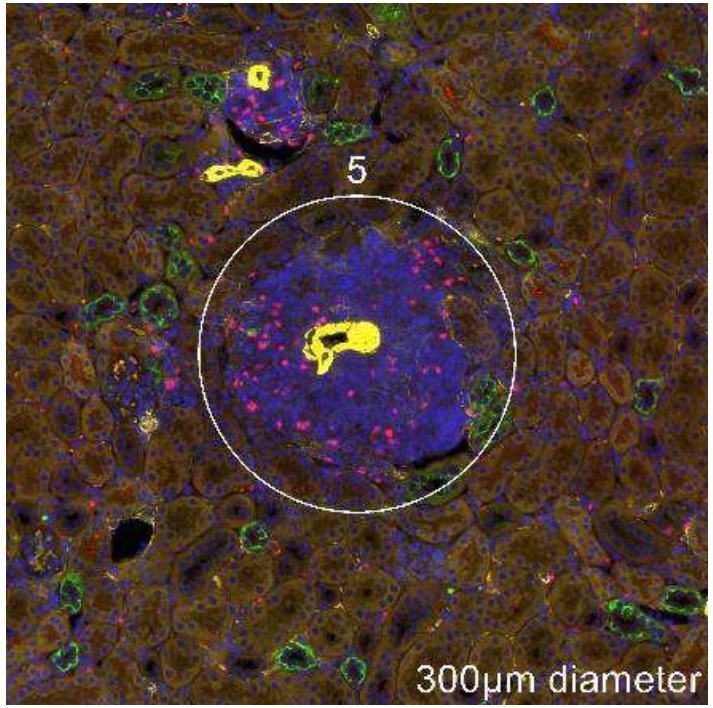

DAPI
Smooth muscle actin
Foxp3
Pan-cytokeratin

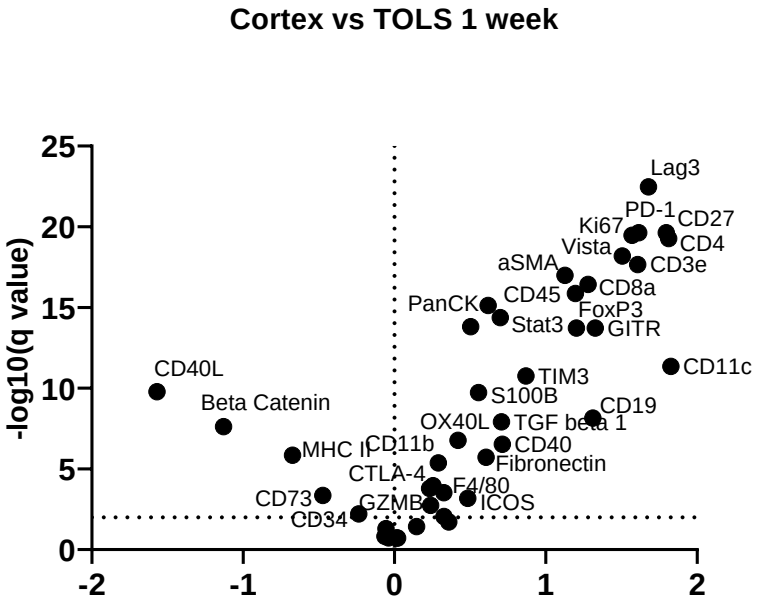

Protein	Difference
Lag3	1.679
CD27	1.795
PD-1	1.614
Ki67	1.569
CD4	1.812
Vista	1.506
CD3e	1.607
aSMA	1.126
CD8a	1.279
CD45	1.195
PanCK	0.6185
Stat3	0.6989
Histone H3	0.5038
FoxP3	1.203
GITR	1.327
CD11c	1.827

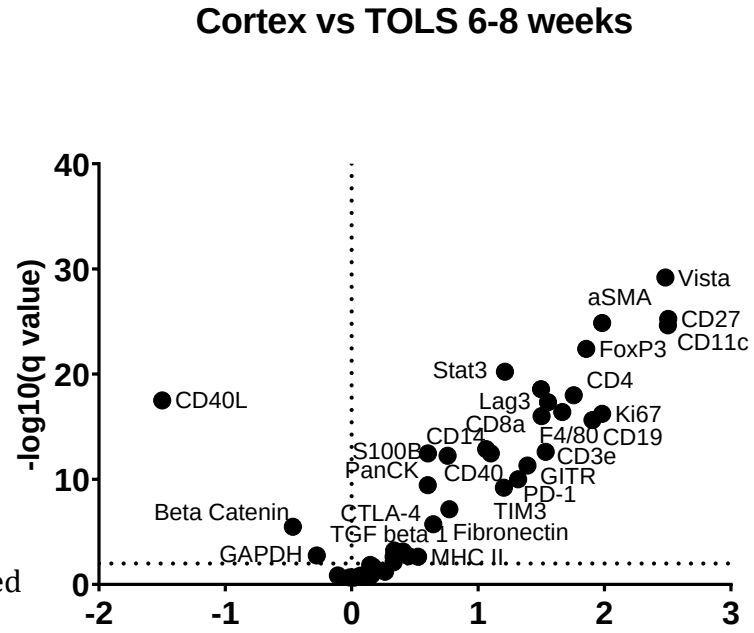

Protein	Difference
Vista	2.482
CD27	2.505
aSMA	1.981
CD11c	2.502
FoxP3	1.855
Stat3	1.212
CD45	1.499
CD4	1.756
CD40L	-1.499
Lag3	1.553
F4/80	1.667
Ki67	1.981
CD8a	1.503
CD19	1.905
CD14	1.063

This article is protected by copyright. All rights reserved

Figure 4

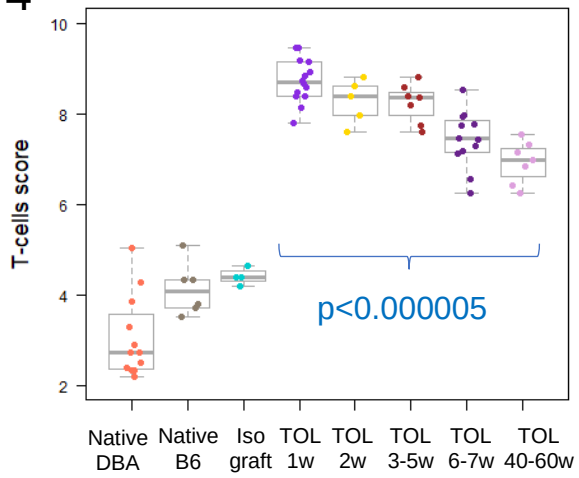

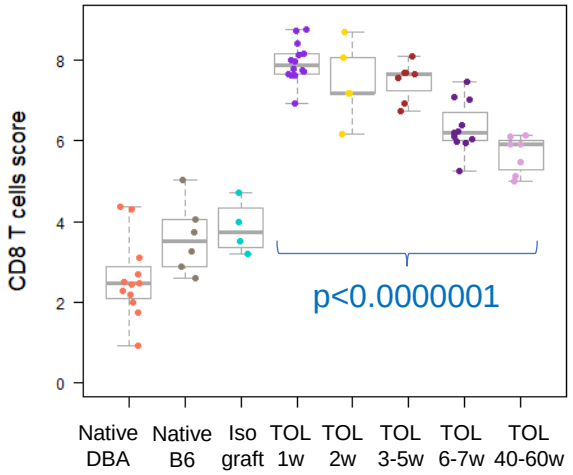

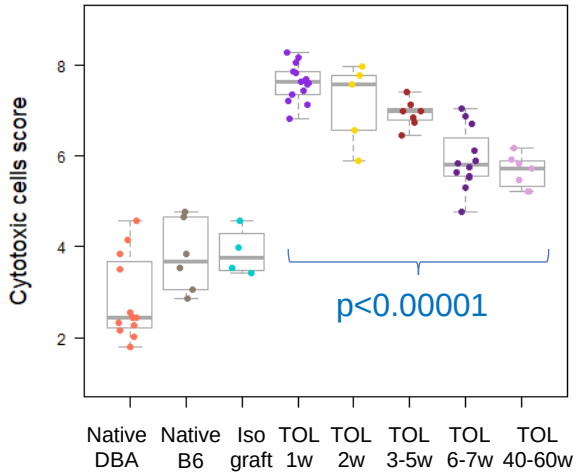

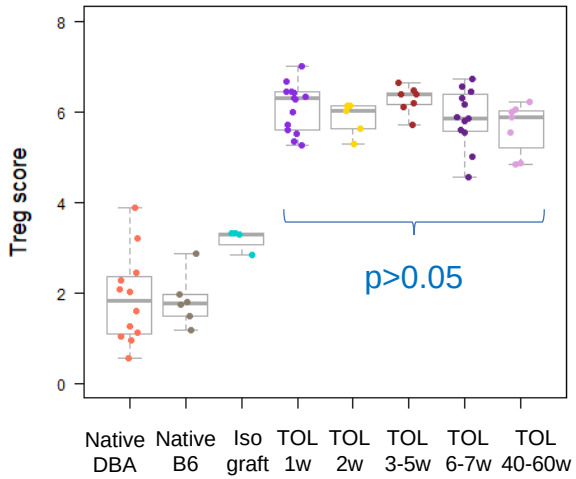

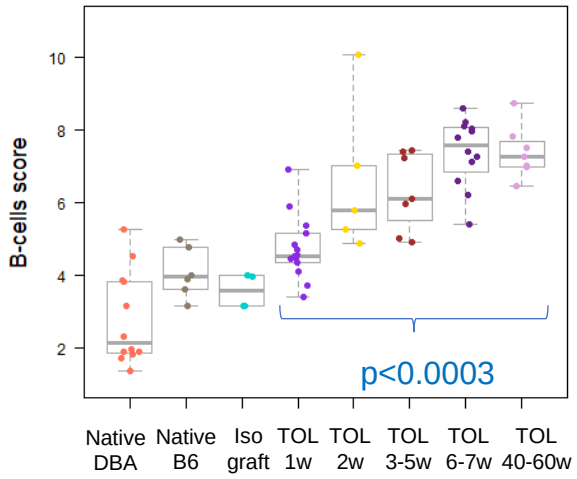

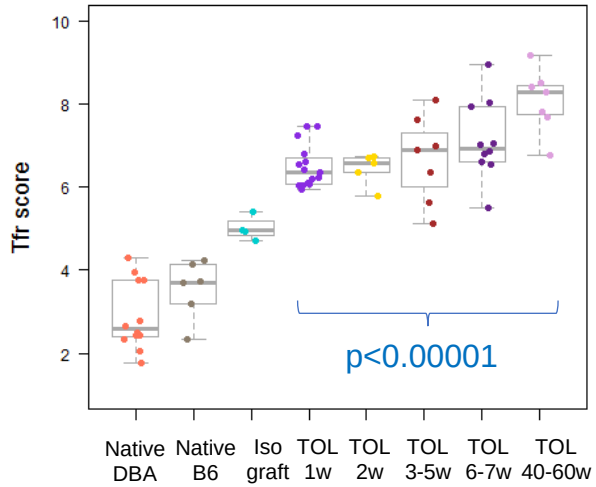

This article is protected by copyright. All rights reserved

Figure 5

Genes increased in rejected grafts (DBA/2 kidneys from C57BL/6 mice) at 1 week

Gene	Log2 fold change	std error (log2)	BY p value
S100a8	-4.43	0.686	9.97E-05
F13a1	-3.58	0.48	1.71E-05
Cxcl14	-3.12	0.327	7.78E-08
H2-Q2	-3.02	0.457	7.14E-05
Cxcl5	-2.66	0.588	0.00743
Ppbp	-2.64	0.444	0.000321
Cd33	-2.58	0.45	0.000547
Ptgs2	-2.58	0.533	0.00382
Nos2	-2.44	0.591	0.0197
Il1b	-2.41	0.592	0.0224
Ccl3	-2.34	0.536	0.011
Lcn2	-2.34	0.584	0.025
Fn1	-2.14	0.382	0.000808
Trem2	-2.03	0.442	0.0065
Msr1	-2.01	0.274	1.72E-05
Clu	-2.01	0.418	0.00382
Amica1	-1.95	0.36	0.0011
Itga5	-1.9	0.361	0.00157
Nlrp3	-1.8	0.374	0.00382
Itgb3	-1.71	0.286	0.000321
Fpr2	-1.66	0.336	0.00339
Clec4n	-1.65	0.355	0.00596
Nod2	-1.62	0.36	0.00767
Col1a1	-1.61	0.325	0.00336
Itgam	-1.58	0.302	0.00161
Fcgr3	-1.49	0.356	0.0165
Thbs1	-1.47	0.332	0.00968
Col3a1	-1.47	0.395	0.0478
Tgfb2	-1.41	0.369	0.0395
Mcam	-1.4	0.283	0.00336
Prf1	-1.39	0.251	0.000959
Lrp1	-1.36	0.314	0.0119
Plaur	-1.28	0.298	0.0123
Anxa1	-1.28	0.313	0.0214
H2-Ea-ps	-1.22	0.324	0.0439
Tlr4	-1.22	0.326	0.047
Lgals3	-1.16	0.24	0.00382
Cdh5	-1.14	0.302	0.0435
Serping1	-1.11	0.24	0.00603
Il4ra	-1.1	0.25	0.0104
Pvr	-1.02	0.215	0.00486
Cd97	-0.987	0.235	0.0164

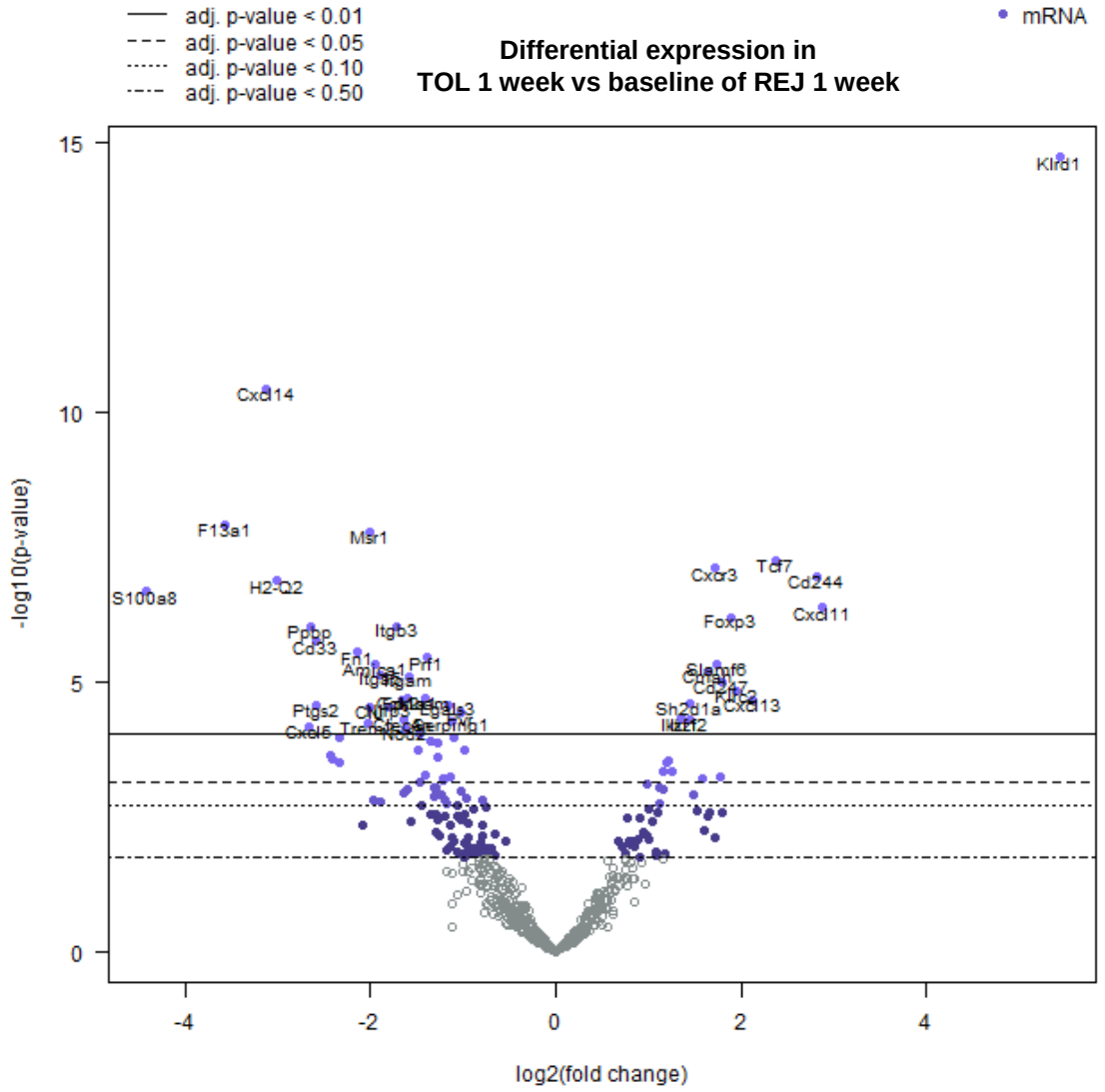

Genes increased in accepted grafts (C57BL/6 kidneys from DBA/2 mice) at 1 week

Gene	Log2 fold change	std error (log2)	BY p value
Klrd1	5.44	0.396	8.13E-12
Cxcl11	2.87	0.46	0.000178
Cd244	2.83	0.423	6.79E-05
Tcf7	2.37	0.342	4.72E-05
Cxcl13	2.13	0.434	0.00339
Klrc2	1.95	0.386	0.00268
Foxp3	1.9	0.312	0.000246
Cd247	1.8	0.346	0.00188
Ctla4	1.77	0.466	0.0421
Slamf6	1.73	0.319	0.0011
Cxcr3	1.71	0.252	5.59E-05
Cmah	1.64	0.308	0.00145
Slamf7	1.58	0.419	0.0439
Sh2d1a	1.45	0.298	0.00372
Ikzf2	1.45	0.314	0.00596
Ikzf1	1.35	0.29	0.00593
Btla	1.26	0.325	0.0364
Tlr1	1.21	0.3	0.0241
Cd83	1.19	0.298	0.025
Cd7	1.16	0.299	0.0361

This article is protected by copyright. All rights reserved

Figure 6

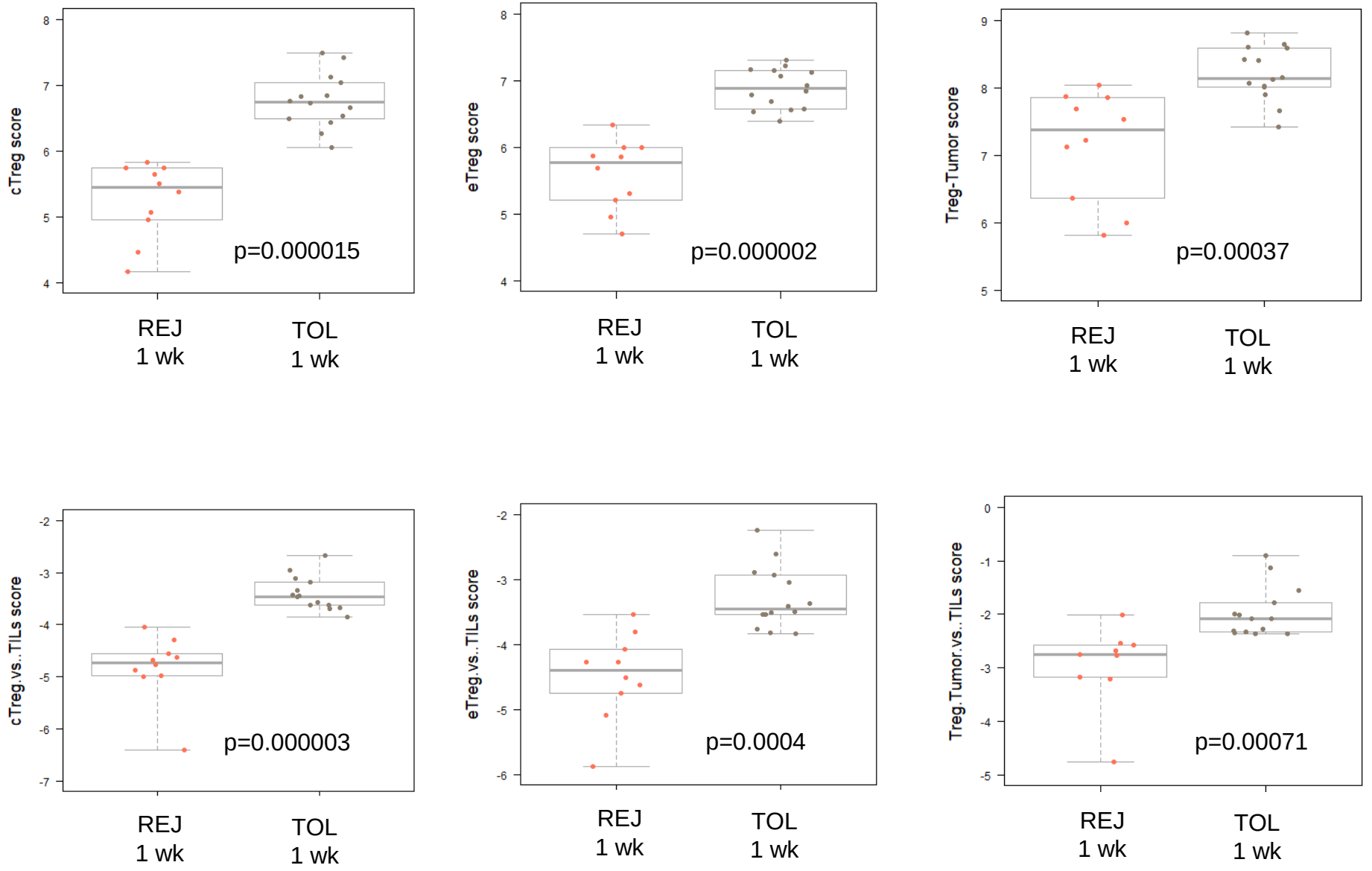

This article is protected by copyright. All rights reserved

Figure 7

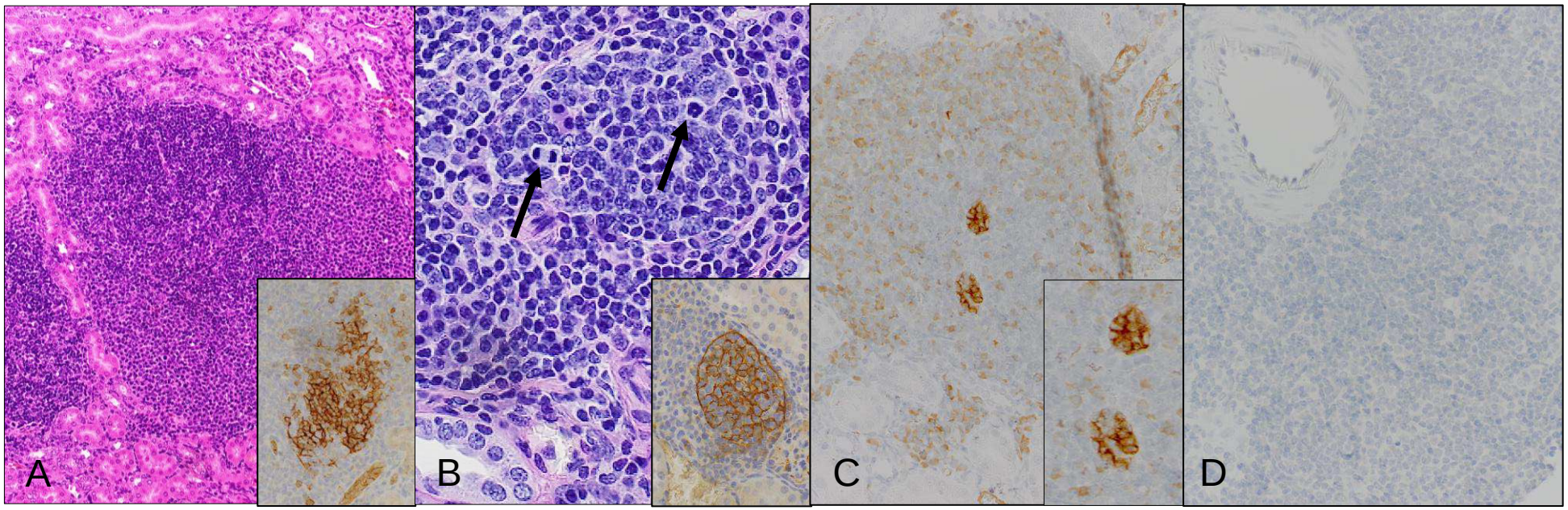

This article is protected by copyright. All rights reserved

Figure 8

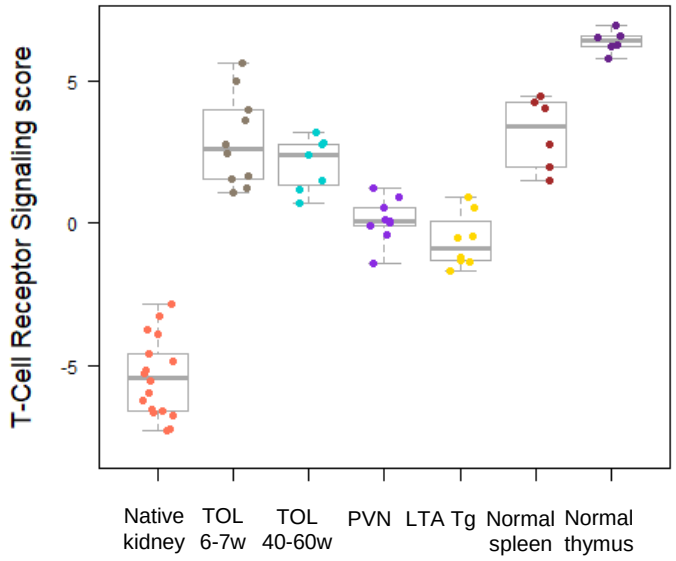

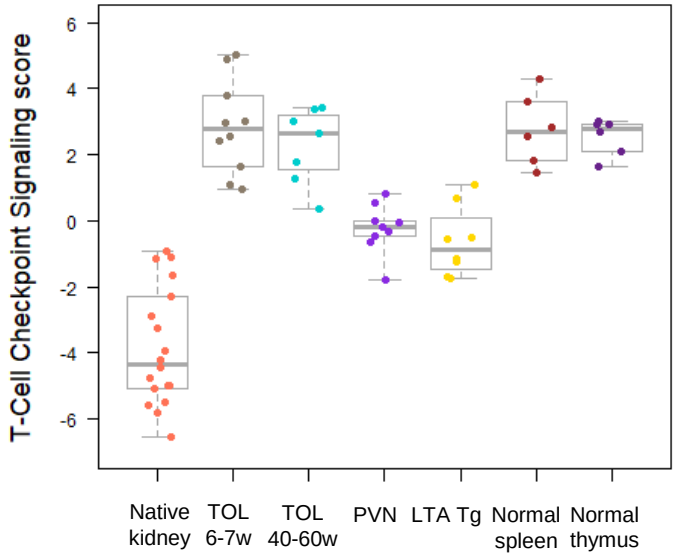

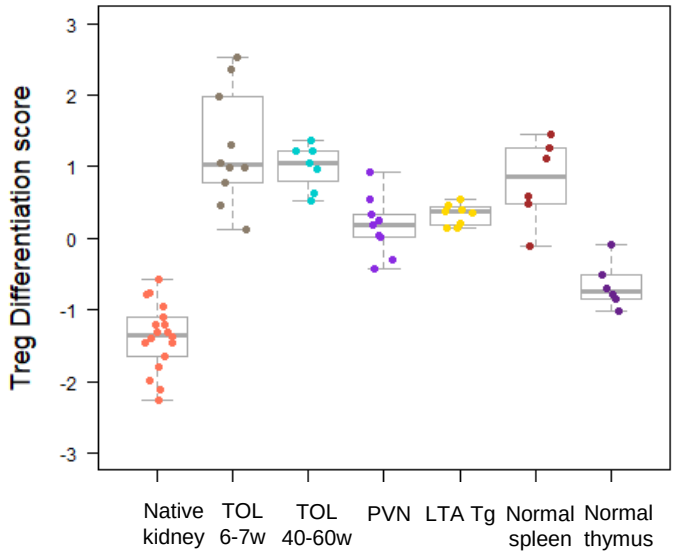

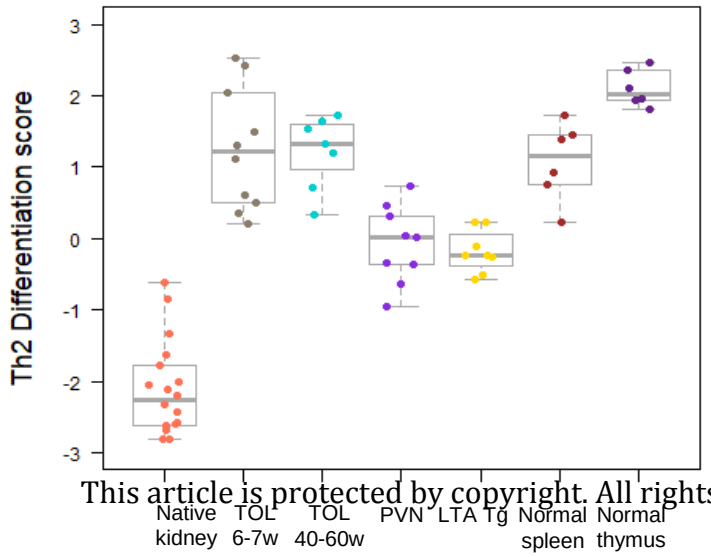

This article is protected by copyright. All rights reserved

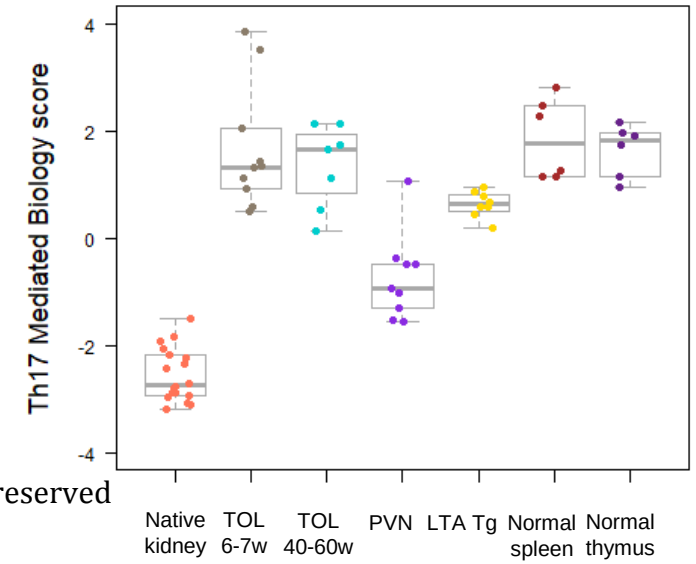

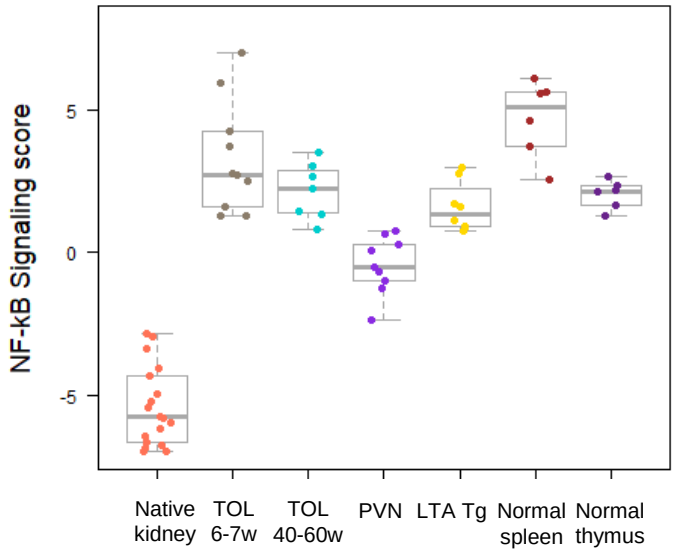

Figure 9

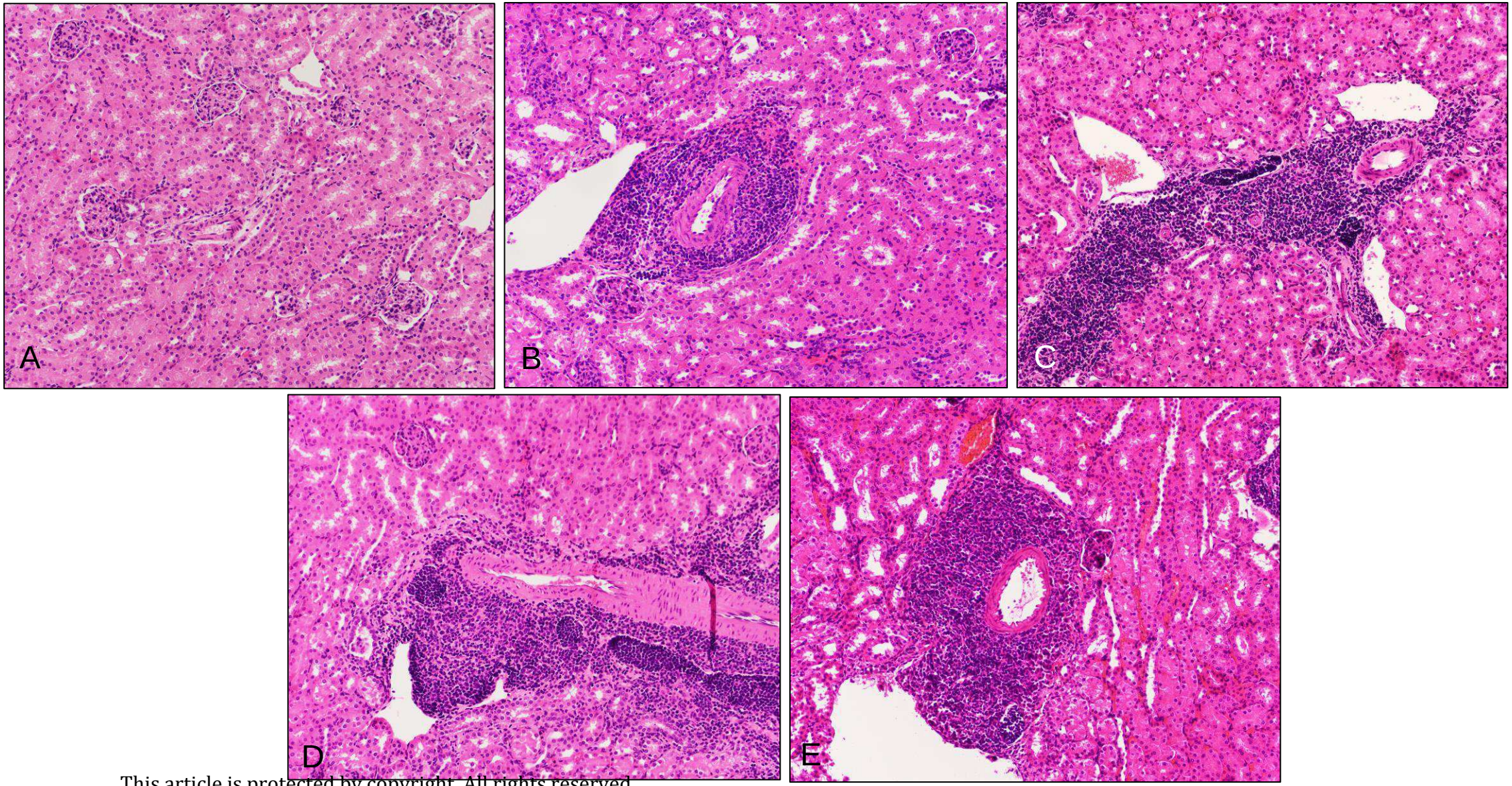

This article is protected by copyright. All rights reserved

Table 1

Table 1. General differences between TOLS and Tertiary Lymphoid Organs (TLOs)

Features	TOLS	TLOs
Location	Spontaneously accepted mouse kidney allografts	Sites of chronic inflammation
Morphology	Periarterial or periarteriolar, appear like sheaths on longitudinal sections	No preferential location; may be associated with mucosal epithelium
Blood vessels	Artery/arteriole	High endothelial venule
Lymphatics	Yes	Yes
B and T cell compartments	No	Yes
Germinal centers	No	Yes
B cell affinity maturation	Unknown	Yes
Cell traffic	Unclear; lymphatics	High endothelial venule
Dependence on LTα signalling	No	Yes
Formation	Independent of secondary lymphoid organs (spleen, lymph nodes and thymus)	In response to chronic inflammation, infection or malignancy

This article is protected by copyright. All rights reserved

Figure 1

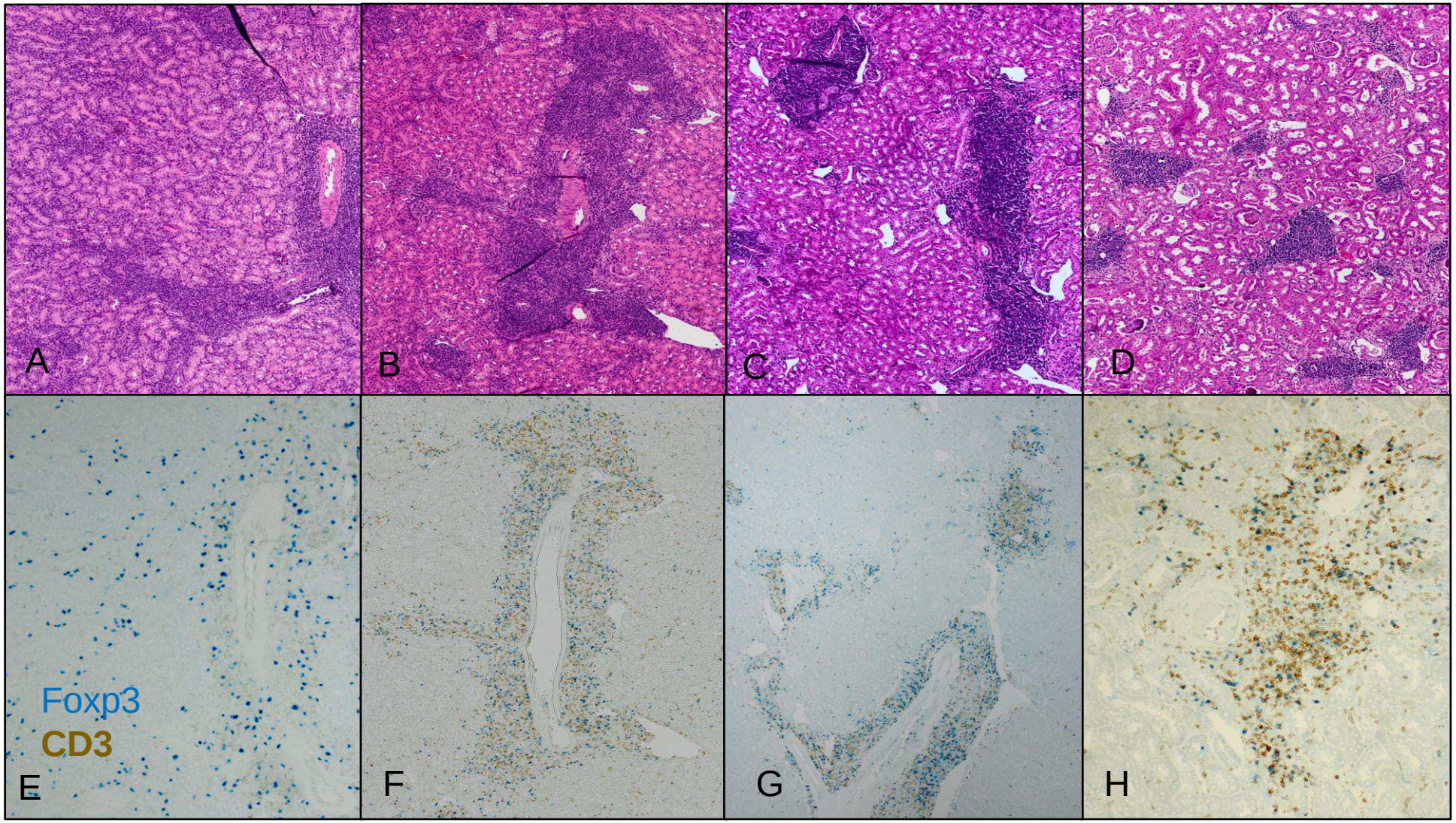

This article is protected by copyright. All rights reserved

Figure 2

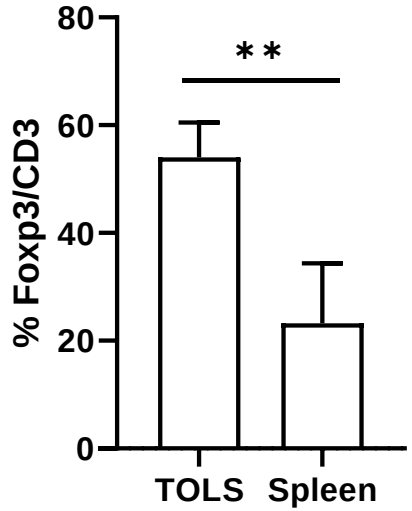

n = 8

A

%Foxp3+CD3+ cells in TOLS and spleens from same recipients

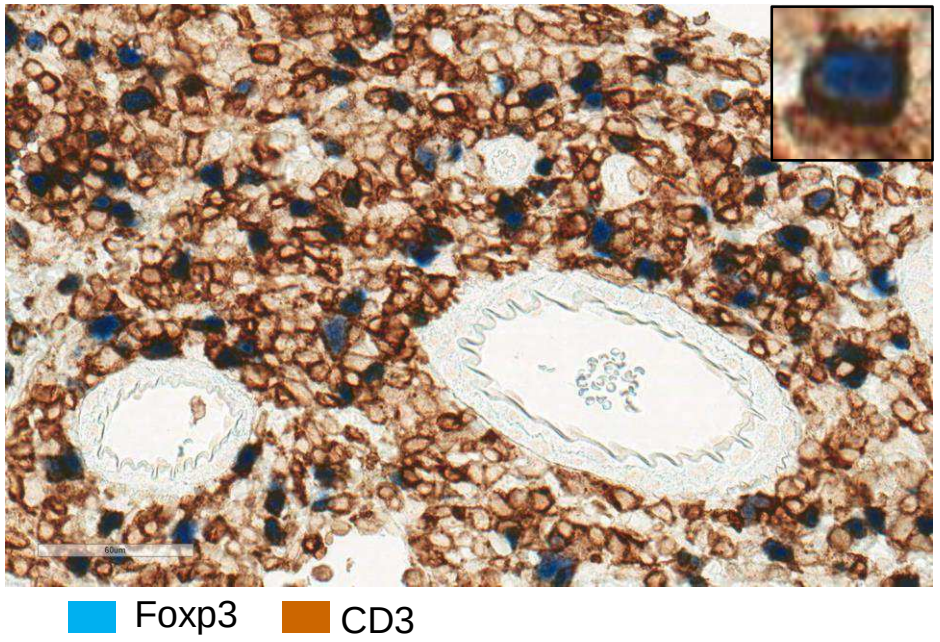

B

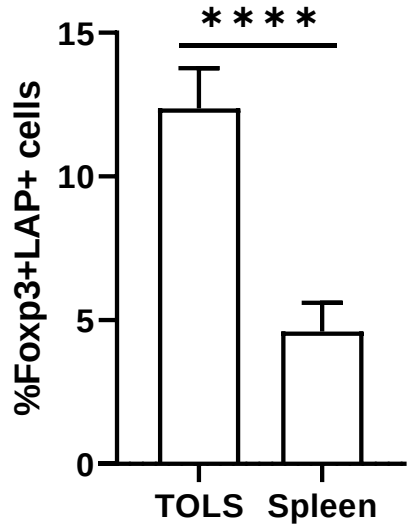

n = 7

C

%Foxp3+LAP+ cells in TOLS and spleens from same recipients

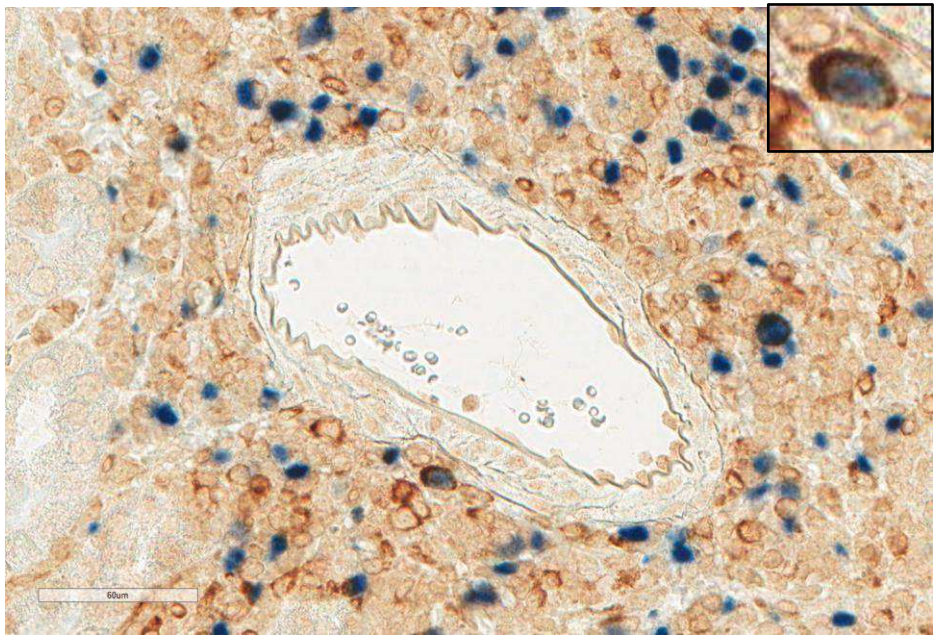

D

This article is protected by copyright. All rights reserved

Figure 3

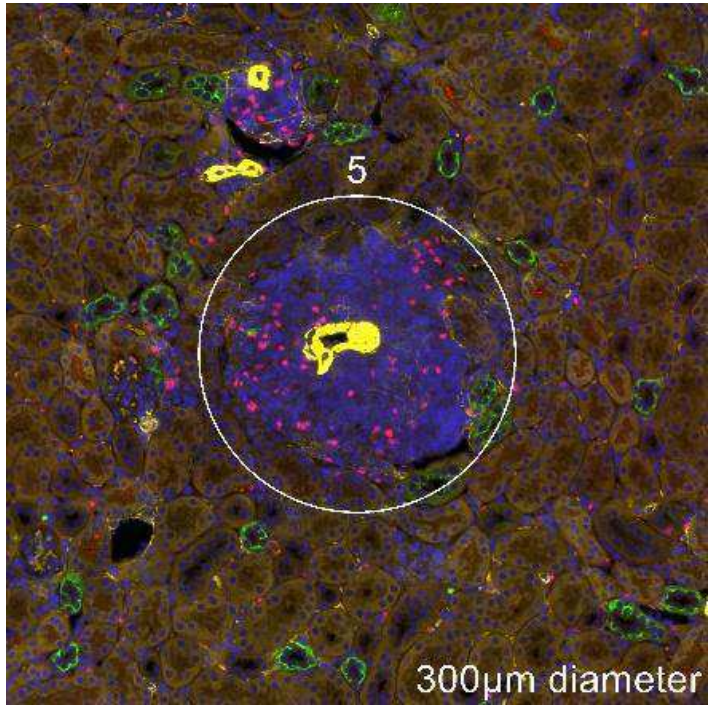

DAPI
Smooth muscle actin
Foxp3
Pan-cytokeratin

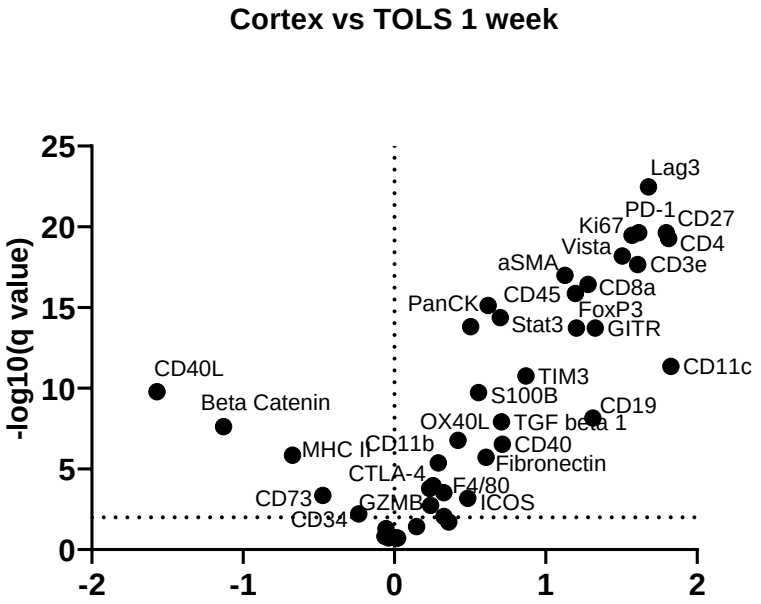

Protein	Difference
Lag3	1.679
CD27	1.795
PD-1	1.614
Ki67	1.569
CD4	1.812
Vista	1.506
CD3e	1.607
aSMA	1.126
CD8a	1.279
CD45	1.195
PanCK	0.6185
Stat3	0.6989
Histone H3	0.5038
FoxP3	1.203
GITR	1.327
CD11c	1.827

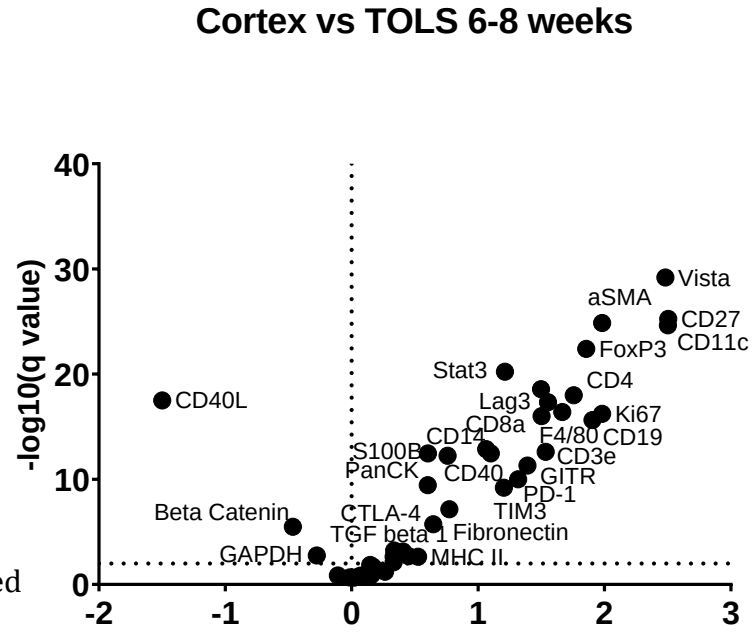

Protein	Difference
Vista	2.482
CD27	2.505
aSMA	1.981
CD11c	2.502
FoxP3	1.855
Stat3	1.212
CD45	1.499
CD4	1.756
CD40L	-1.499
Lag3	1.553
F4/80	1.667
Ki67	1.981
CD8a	1.503
CD19	1.905
CD14	1.063

This article is protected by copyright. All rights reserved

Figure 4

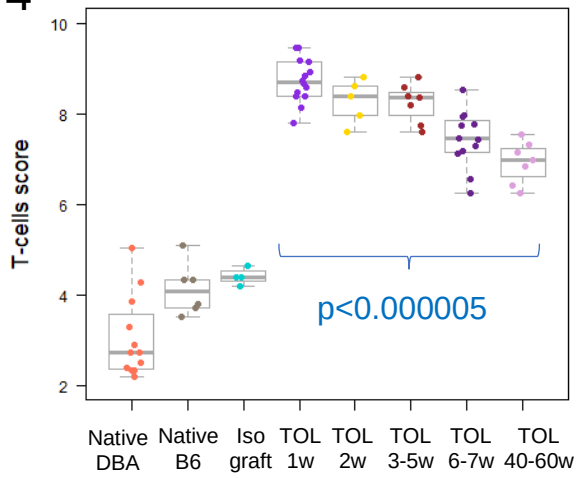

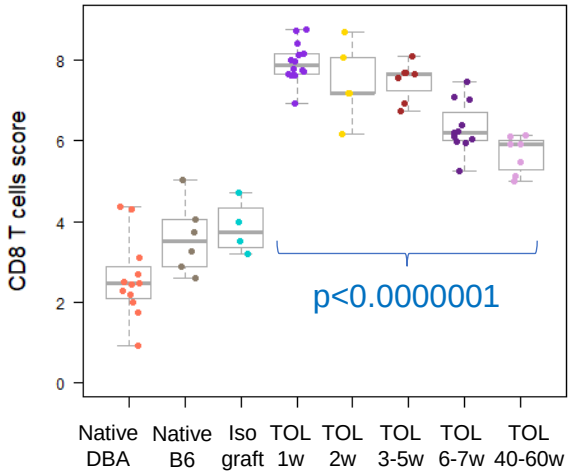

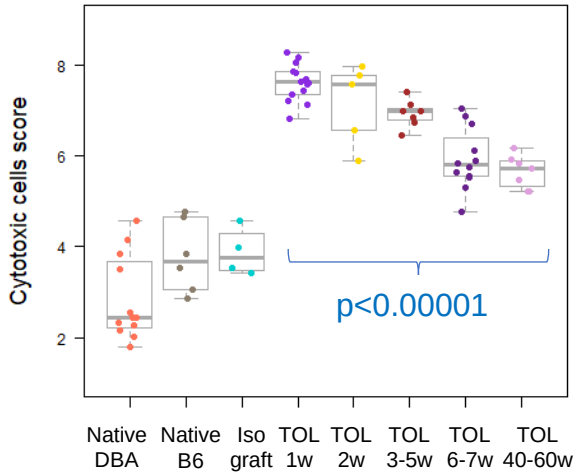

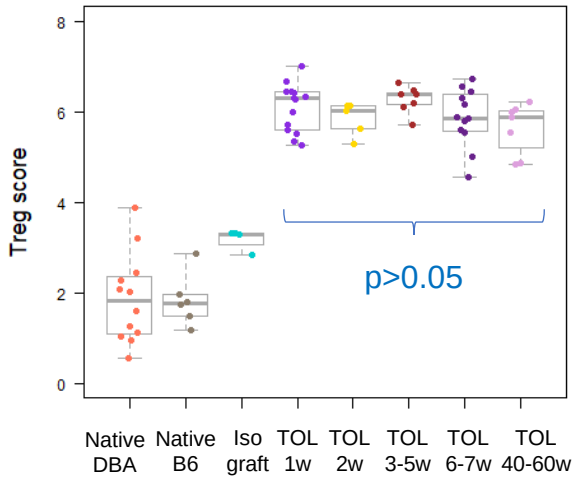

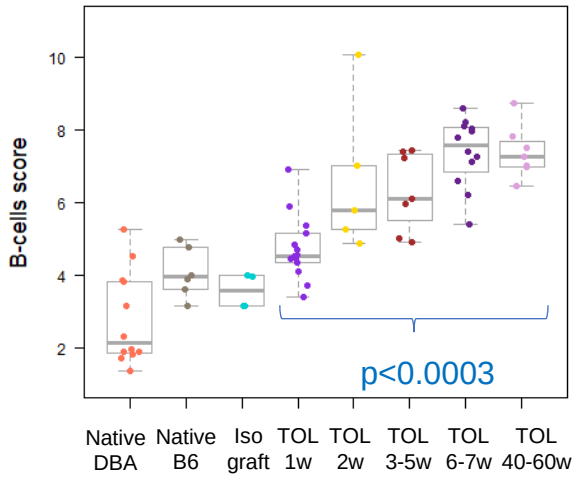

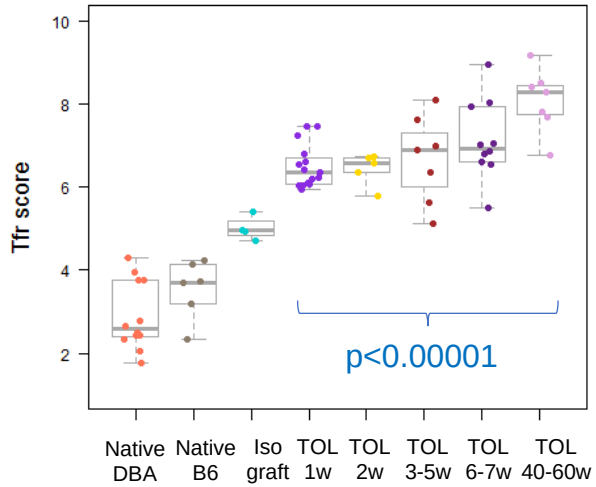

This article is protected by copyright. All rights reserved

Figure 5

Genes increased in rejected grafts (DBA/2 kidneys from C57BL/6 mice) at 1 week

Gene	Log2 fold change	std error (log2)	BY p value
S100a8	-4.43	0.686	9.97E-05
F13a1	-3.58	0.48	1.71E-05
Cxcl14	-3.12	0.327	7.78E-08
H2-Q2	-3.02	0.457	7.14E-05
Cxcl5	-2.66	0.588	0.00743
Ppbp	-2.64	0.444	0.000321
Cd33	-2.58	0.45	0.000547
Ptgs2	-2.58	0.533	0.00382
Nos2	-2.44	0.591	0.0197
Il1b	-2.41	0.592	0.0224
Ccl3	-2.34	0.536	0.011
Lcn2	-2.34	0.584	0.025
Fn1	-2.14	0.382	0.000808
Trem2	-2.03	0.442	0.0065
Msr1	-2.01	0.274	1.72E-05
Clu	-2.01	0.418	0.00382
Amica1	-1.95	0.36	0.0011
Itga5	-1.9	0.361	0.00157
Nlrp3	-1.8	0.374	0.00382
Itgb3	-1.71	0.286	0.000321
Fpr2	-1.66	0.336	0.00339
Clec4n	-1.65	0.355	0.00596
Nod2	-1.62	0.36	0.00767
Col1a1	-1.61	0.325	0.00336
Itgam	-1.58	0.302	0.00161
Fcgr3	-1.49	0.356	0.0165
Thbs1	-1.47	0.332	0.00968
Col3a1	-1.47	0.395	0.0478
Tgfb2	-1.41	0.369	0.0395
Mcam	-1.4	0.283	0.00336
Prf1	-1.39	0.251	0.000959
Lrp1	-1.36	0.314	0.0119
Plaur	-1.28	0.298	0.0123
Anxa1	-1.28	0.313	0.0214
H2-Ea-ps	-1.22	0.324	0.0439
Tlr4	-1.22	0.326	0.047
Lgals3	-1.16	0.24	0.00382
Cdh5	-1.14	0.302	0.0435
Serping1	-1.11	0.24	0.00603
Il4ra	-1.1	0.25	0.0104
Pvr	-1.02	0.215	0.00486
Cd97	-0.987	0.235	0.0164

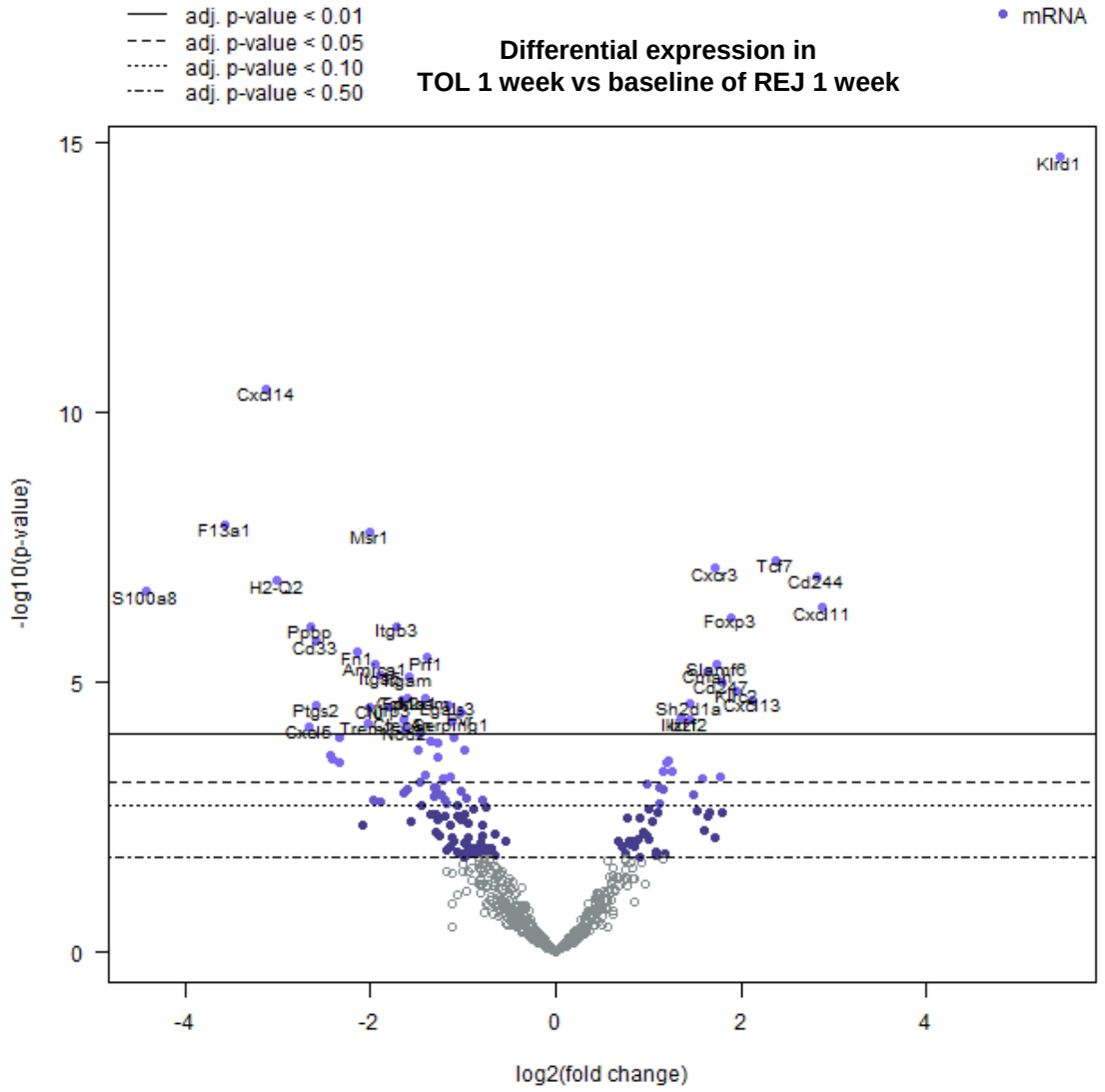

Genes increased in accepted grafts (C57BL/6 kidneys from DBA/2 mice) at 1 week

Gene	Log2 fold change	std error (log2)	BY p value
Klrd1	5.44	0.396	8.13E-12
Cxcl11	2.87	0.46	0.000178
Cd244	2.83	0.423	6.79E-05
Tcf7	2.37	0.342	4.72E-05
Cxcl13	2.13	0.434	0.00339
Klrc2	1.95	0.386	0.00268
Foxp3	1.9	0.312	0.000246
Cd247	1.8	0.346	0.00188
Ctla4	1.77	0.466	0.0421
Slamf6	1.73	0.319	0.0011
Cxcr3	1.71	0.252	5.59E-05
Cmah	1.64	0.308	0.00145
Slamf7	1.58	0.419	0.0439
Sh2d1a	1.45	0.298	0.00372
Ikzf2	1.45	0.314	0.00596
Ikzf1	1.35	0.29	0.00593
Btla	1.26	0.325	0.0364
Tlr1	1.21	0.3	0.0241
Cd83	1.19	0.298	0.025
Cd7	1.16	0.299	0.0361

This article is protected by copyright. All rights reserved

Figure 6

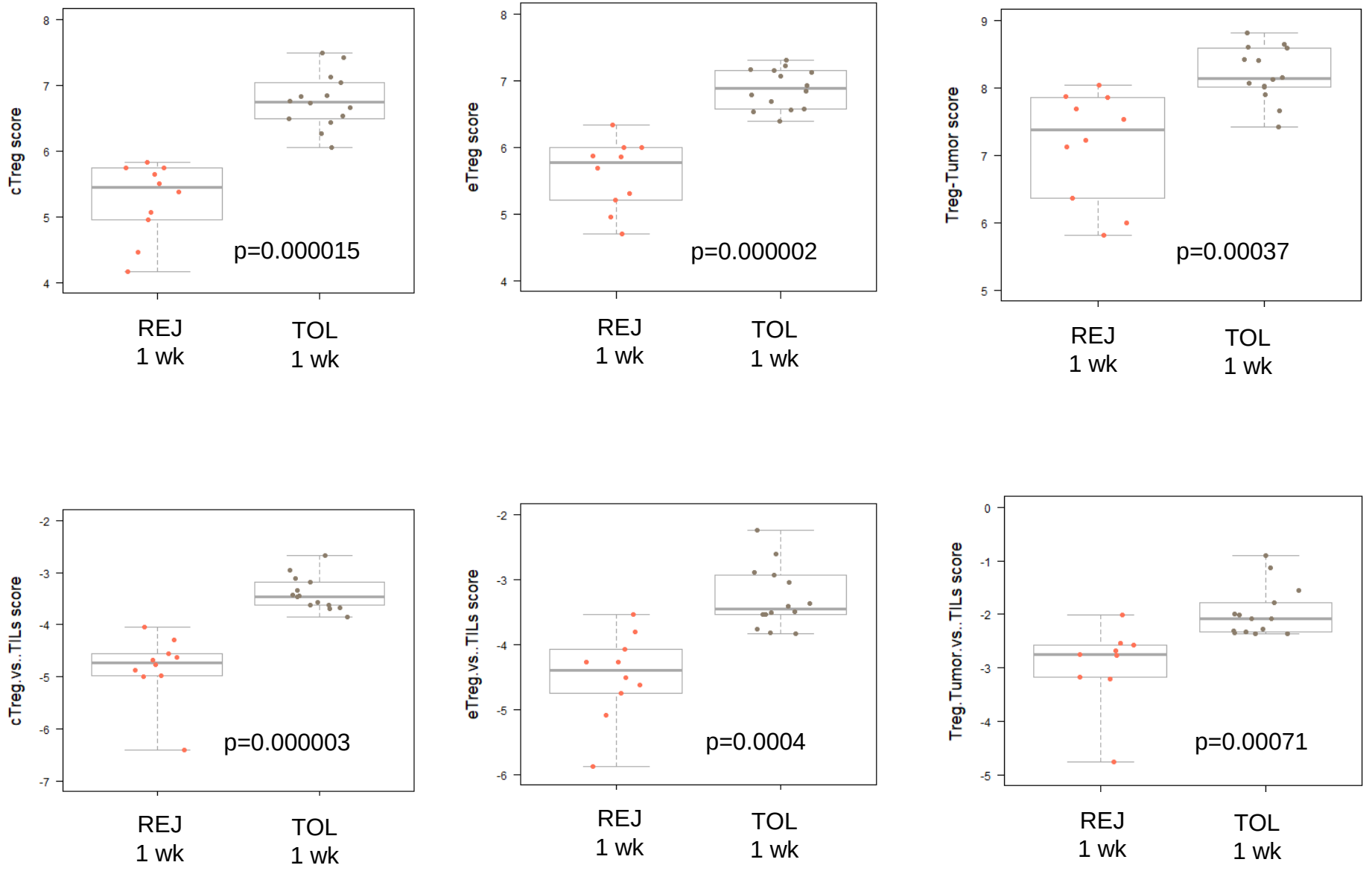

This article is protected by copyright. All rights reserved

Figure 7

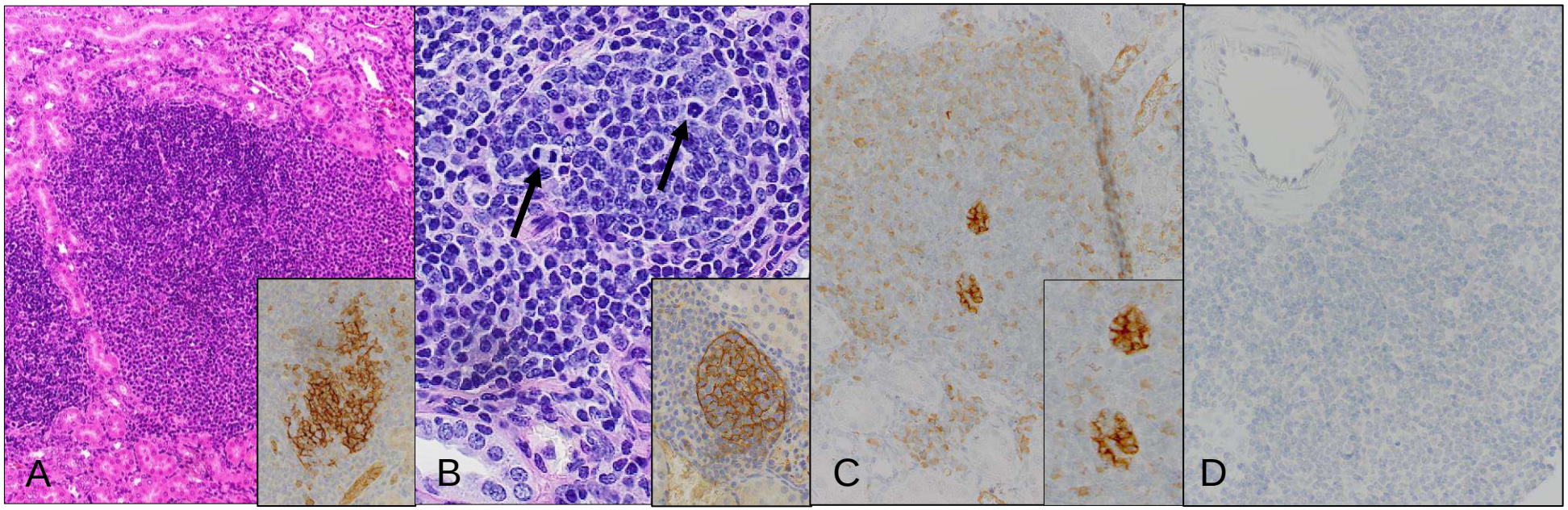

This article is protected by copyright. All rights reserved

Figure 8

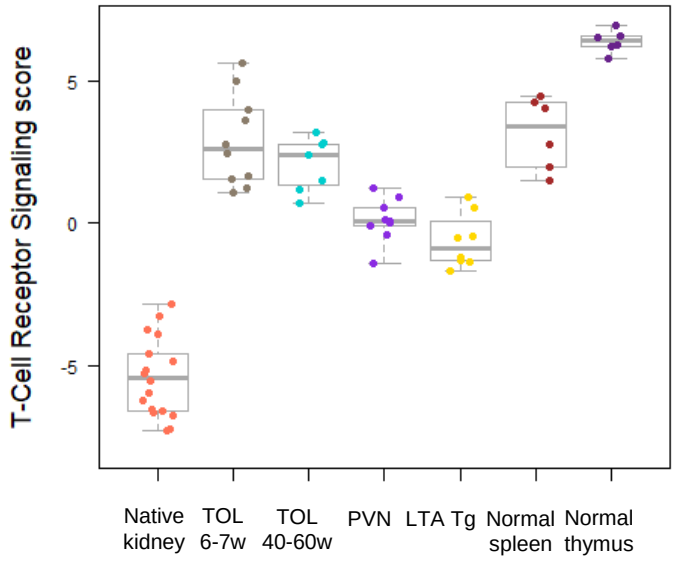

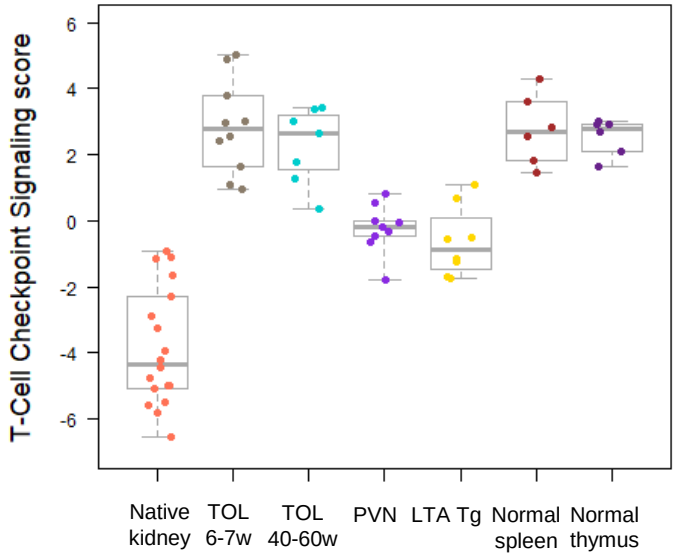

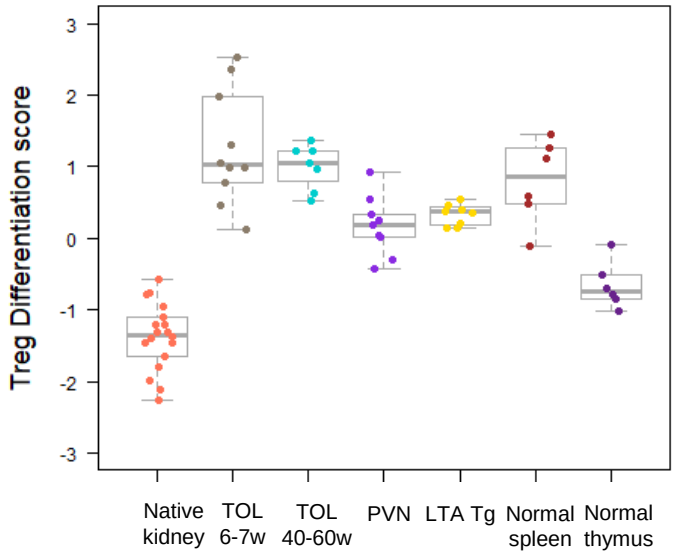

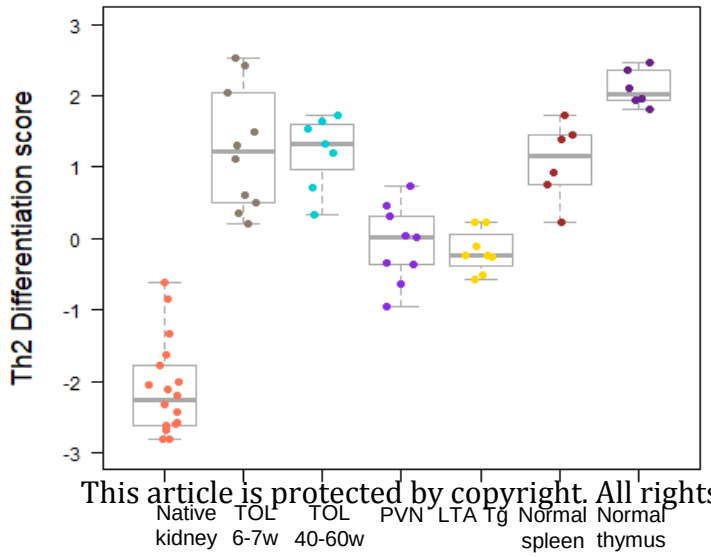

This article is protected by copyright. All rights reserved

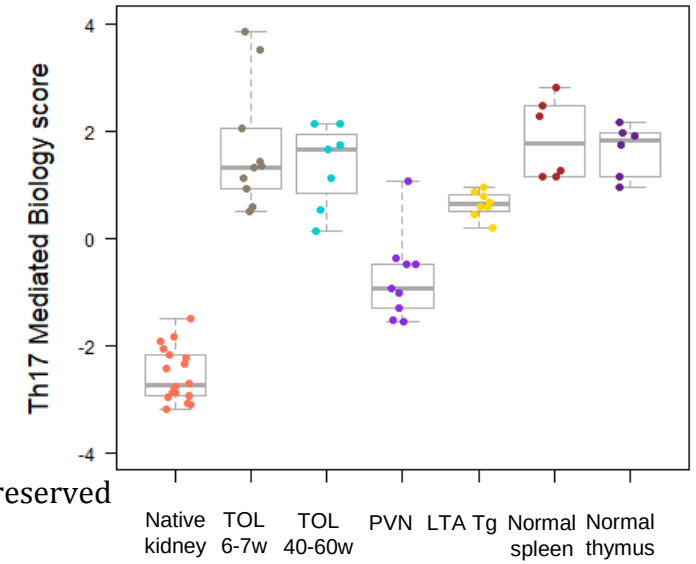

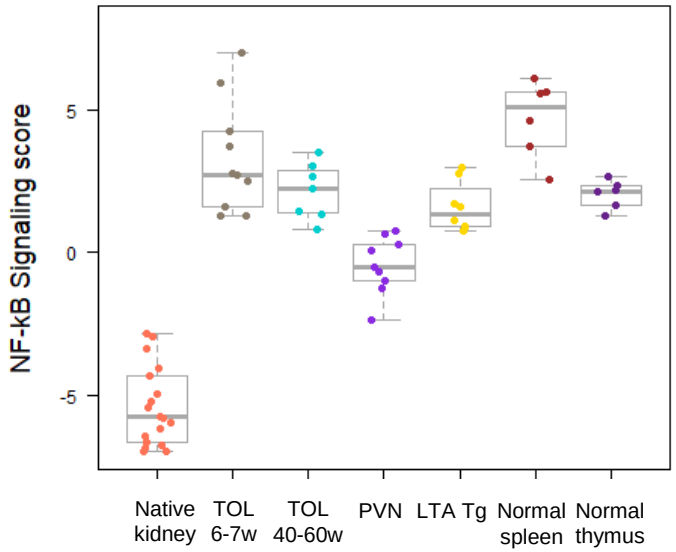

Figure 9

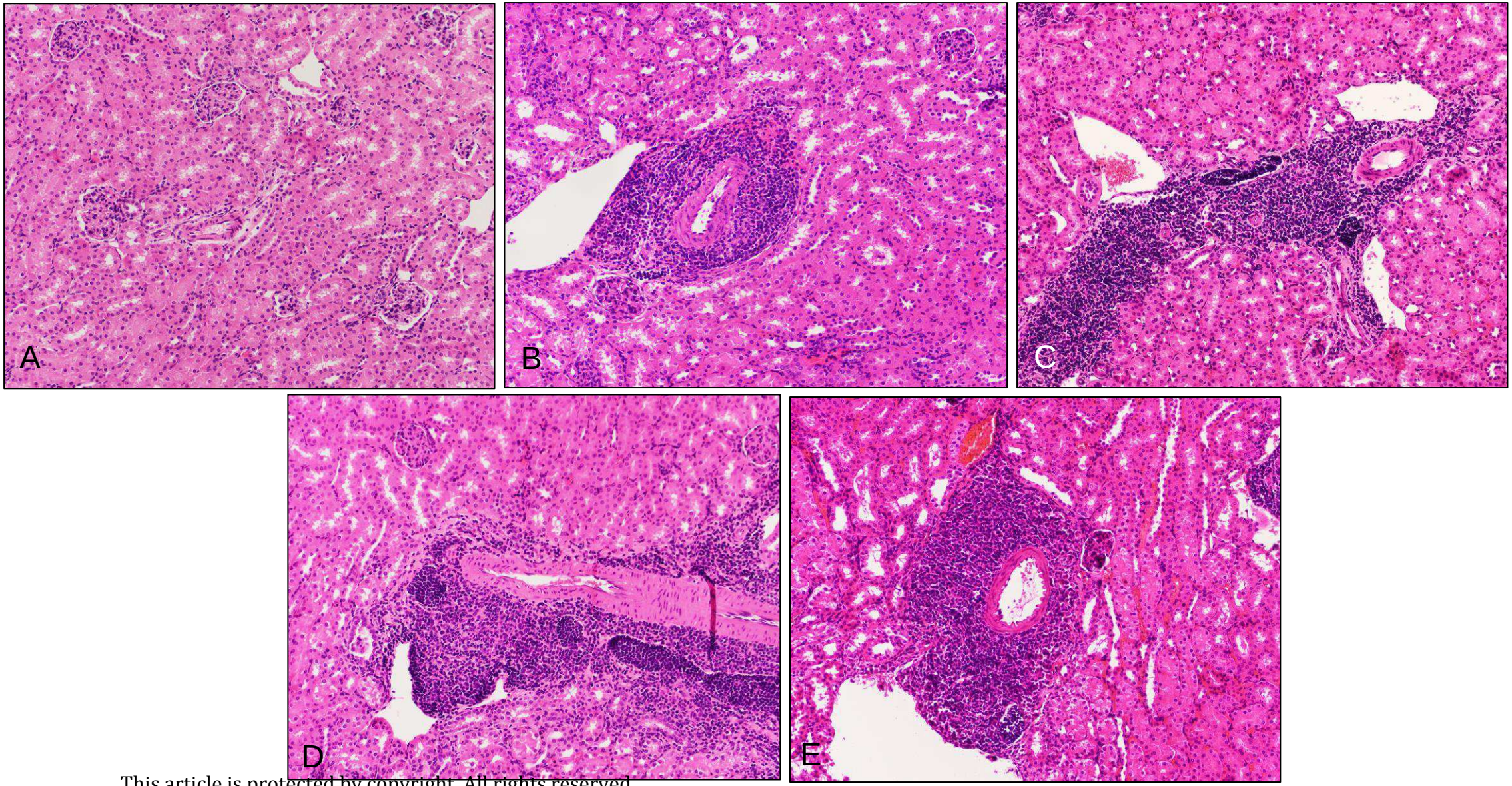

This article is protected by copyright. All rights reserved

Table 1

Table 1. General differences between TOLS and Tertiary Lymphoid Organs (TLOs)

Features	TOLS	TLOs
Location	Spontaneously accepted mouse kidney allografts	Sites of chronic inflammation
Morphology	Periarterial or periarteriolar, appear like sheaths on longitudinal sections	No preferential location; may be associated with mucosal epithelium
Blood vessels	Artery/arteriole	High endothelial venule
Lymphatics	Yes	Yes
B and T cell compartments	No	Yes
Germinal centers	No	Yes
B cell affinity maturation	Unknown	Yes
Cell traffic	Unclear; lymphatics	High endothelial venule
Dependence on LTα signalling	No	Yes
Formation	Independent of secondary lymphoid organs (spleen, lymph nodes and thymus)	In response to chronic inflammation, infection or malignancy

This article is protected by copyright. All rights reserved